

**UNIVERSIDADE FEDERAL DE SANTA CATARINA  
DEPARTAMENTO DE ENGENHARIA MECÂNICA**

Henrique dos Santos Carminatti

**SIMULATION AND TEST OF A SOLAR DOMESTIC  
WATER HEATING SYSTEM CONTROLLED BY  
WEATHER FORECAST INFORMATION.**

Florianópolis

2017

Henrique dos Santos Carminatti

**SIMULATION AND TEST OF A SOLAR DOMESTIC  
WATER HEATING SYSTEM CONTROLLED BY  
WEATHER FORECAST INFORMATION.**

Dissertação submetida ao Programa  
de Pós-Graduação em Engenharia Me-  
cânica para a obtenção do Grau de  
Mestre em Engenharia e Ciências Tér-  
micas.

Orientador: Prof. Dr. Sergio Colle

Florianópolis

2017



Ficha de identificação da obra elaborada pelo autor,  
através do Programa de Geração Automática da Biblioteca Universitária da UFSC.

Carminatti, Henrique  
Simulation and Test of a Solar Domestic Water  
Heating System Controlled by Weather Forecast  
Information / Henrique Carminatti ; orientador,  
Sergio Colle, 2017.  
119 p.

Dissertação (mestrado) - Universidade Federal de  
Santa Catarina, , Programa de Pós-Graduação em  
Engenharia Mecânica, Florianópolis, 2017.

Inclui referências.

1. Engenharia Mecânica. 2. Aquecimento Solar para  
uso doméstico. 3. Controle por informação  
meteorológica de meso escal. 4. Validação  
experimental. I. Colle, Sergio. II. Universidade  
Federal de Santa Catarina. Programa de Pós-Graduação  
em Engenharia Mecânica. III. Título.

Henrique dos Santos Carminatti

**SIMULATION AND TEST OF A SOLAR DOMESTIC  
WATER HEATING SYSTEM CONTROLLED BY  
WEATHER FORECAST INFORMATION.**

Esta Dissertação foi julgada aprovada para a obtenção do Título de “Mestre em Engenharia e Ciências Térmicas”, e aprovada em sua forma final pelo Programa de Pós-Graduação em Engenharia Mecânica.

Florianópolis, 24 de Agosto 2017.

---

Prof. Dr. Jonny Carlos da Silva  
Coordenador do Curso

---

Prof. Dr. Sergio Colle  
Orientador

**Banca Examinadora:**

---

Prof. Antônio Fábio Carvalho da Silva  
Presidente

---

Prof. Amir Antonio Martins Oliveira Jr.

---

Prof. Samuel Luna de Abreu



Dedico este trabalho ao meu pai Álvaro  
Carminatti



## AGRADECIMENTOS

Inicialmente devo agradecer a minha família por sempre me apoiarem em minhas empreitadas. Agradeço também a minha namorada por me ajudar em todos os momentos de necessidade. Agradeço aos meus amigos e colegas de laboratório, em especial ao Theo Doria Motin Ruas por ter me ajudado a montar a bancada de testes de baixo de sol e muito calor, em especial também a Alan Starke por me ajudar a compilar e analisar os resultados.

Agradeço aos membros da banca por analisarem meu trabalho com atenção, em especial ao Professor Samuel Luna de Abreu. Agradeço ao meu orientador pela oportunidade e experiência de trabalhar no laboratório de energia Solar por 7 anos. Em verdade muitos foram os que me ajudaram neste trabalho e seria quase impossível colocar o nome de todos aqui, mais difícil ainda seria sintetizar a ajuda de cada um em palavras. Resumo tudo a um grande muito obrigado, e a promessa de que cada um que precise da minha ajuda também a receberá de bom grado assim como fizeram comigo.



*39,847 is a prime number, and, believe it or not, 48,099,473 also is.*

Research Findings





## SUMÁRIO

|  |       |
|--|-------|
| Resumo .....   | xiii  |
| Resumo Expandido.....  | xv    |
| Abstract .....   | xvii  |
| Lista de Figuras .....   | xxi   |
| Lista de Tabelas .....   | xxiii |
| Lista de Abreviaturas e Siglas.....  | xxv   |
| Lista de Símbolos .....  | xxvii |
| 1 INTRODUCTION .....   | 1     |
| 2 BACKGROUND AND LITERATURE REVIEW .....   | 5     |
| 2.1 SOLAR SYSTEMS SIMULATION AND DATA SERIES.....  | 5     |
| 2.1.1 Climatic Variables and simulated Weather Forecast<br>Errors .....                        | 6     |
| 2.1.1.1 Synthetic Data-sets .....  | 7     |
| 2.2 WEATHER FORECAST CONTROLLED SOLAR ENERGY<br>SYSTEMS .....                                  | 8     |
| 2.2.0.1 Weather and Load Forecast .....  | 9     |
| 2.2.0.2 Modern Weather and Load forecast Strategy .....  | 10    |
| 2.2.1 Starting point of the PSDWHS .....   | 10    |
| 2.2.2 Design of the PSDWHS.....  | 11    |
| 2.2.3 System effectiveness measurement .....   | 11    |
| 2.2.3.1 Simulation of the PSDWHS: Equal Days Strategy for<br>Florianopolis .....               | 12    |
| 2.2.3.2 Simulation of the PSDWHS: Simulated Weather Forecast<br>Errors for Florianopolis ..... | 12    |
| 3 SDWHS AND SIMULATION .....   | 15    |
| 3.1 COMPUTATIONAL ANALYSIS.....  | 16    |
| 3.2 THE PROPOSED CONTROL STRATEGIES AND SIMU-<br>LATED WEATHER FORECAST ERRORS.....            | 17    |
| 3.2.1 Simulation Control Strategy 1: Equal Days .....  | 18    |
| 3.2.2 Simulation Control Strategy 2: Weather Forecast.....                                     | 18    |
| 3.2.3 Load Profile .....   | 21    |
| 4 FULL SCALE EXPERIMENT.....   | 23    |
| 4.1 TEST BED APPARATUS .....   | 23    |
| 4.1.1 Structure and Basic Devices .....  | 24    |
| 4.1.1.1 Tanks .....  | 24    |
| 4.1.1.2 Auxiliary Heaters .....  | 25    |
| 4.1.1.3 Collectors.....  | 25    |
| 4.1.1.4 Water Filter .....   | 25    |

|  |           |
|--|-----------|
| 4.1.1.5 Pull and Outside Electronics Boxes .....   | 26        |
| <b>4.1.2 Measurement Equipments .....</b>  | <b>27</b> |
| 4.1.2.1 Temperature Transducers .....  | 27        |
| 4.1.2.2 Solar Radiation Transducer .....   | 28        |
| 4.1.2.3 Flow Meter .....   | 28        |
| <b>4.1.3 System Control Apparatus .....</b>  | <b>29</b> |
| 4.1.3.1 Solenoid Valves .....  | 29        |
| 4.1.3.2 Arduino .....  | 29        |
| 4.1.3.3 Agilent 34972A Data-logger .....   | 30        |
| <b>4.1.4 System Control Procedure .....</b>  | <b>30</b> |
| <b>4.2 EXPERIMENTAL DATA .....</b>   | <b>31</b> |
| <b>4.2.1 Simulation Validation .....</b>   | <b>31</b> |
| 4.2.1.1 Backup Tank validation: Type 533 .....   | 32        |
| 4.2.1.2 Collector Tank Validation: Type 45a part 1 .....                                   | 35        |
| 4.2.1.3 Collector Validation: Type 45a part 2 .....  | 36        |
| 4.2.1.4 Simulated System Validation .....  | 38        |
| <b>5 SIMULATION RESULTS .....</b>  | <b>47</b> |
| <b>5.1 FLORIANOPOLIS .....</b>   | <b>47</b> |
| <b>5.1.1 Florianopolis previous day strategy and weather fo-<br/>recast strategy .....</b> | <b>47</b> |
| <b>5.2 RESULTS FOR OTHER CITIES .....</b>  | <b>49</b> |
| <b>5.2.1 Koller’s Control Strategy .....</b>   | <b>49</b> |
| <b>5.2.2 Weather Forecast Strategy .....</b>   | <b>52</b> |
| <b>6 CONCLUSIONS FUTURE WORKS AND SUGGES-<br/>TIONS.....</b>                               | <b>61</b> |
| <b>REFERÊNCIAS .....</b>   | <b>63</b> |
| <b>APÊNDICE A – Test Bed Hydraulic Design .....</b>  | <b>70</b> |
| <b>APÊNDICE B – Test Bed Electric Design .....</b>   | <b>73</b> |
| <b>APÊNDICE C – Labview: System Control Procedure ..</b>                                   | <b>77</b> |
| <b>ANEXO A – Temperature Transducers Calibration by<br/>Oestreich (2017) .....</b>         | <b>85</b> |

## RESUMO

O Brasil possui uma vasta diversidade de fontes energéticas. De grandes hidrelétricas, as quais são sua fonte principal, até os mais recentes parques eólicos e fotovoltaicos. No entanto, a despeito desta variedade de recursos energéticos há uma verdade negativa: a maioria das habitações no país usa chuveiros elétricos. Esses dispositivos são responsáveis por 43% do pico de demanda de energia elétrica doméstico Brasileiro. Esse pico de demanda de energia causa problemas não só à companhia geradora de energia, a qual tem que reservar pelo menos quatro giga watts para fornecê-lo, mas também para a empresa de distribuição de energia elétrica devido à sobrecarga e/ou superdimensionamento de cabos e danos aos transformadores.

Com o objetivo de transferir o uso de energia elétrica para aquecimento de água para o amanhecer, um novo Sistema de Aquecimento Solar de Água Doméstico foi simulado e testado. O objetivo deste sistema é planificar o perfil de consumo de energia elétrica de uma casa. Este sistema usa dois tanques e dados de previsão do tempo para prever a energia solar absorvida pelo coletor para o próximo dia, a fim de evitar possíveis condições climáticas desfavoráveis. A análise computacional foi realizada utilizando o software TRNSYS.

O sistema apresentado foi capaz de diminuir o pico da demanda de energia elétrica. As simulações forneceram dados esperados e provaram que o sistema pode ser usado em muitas regiões brasileiras, mudando o pico de demanda de energia de uma habitação. No entanto, à medida que os erros de previsão simulados aumentaram, o sistema não conseguiu fornecer água quente ao usuário com mais frequência. Mais pesquisas são necessárias para rastrear uma tendência para justificar um ponto de parada para o aumento da precisão da previsão do tempo. Além disso, para validar a simulação, uma bancada de testes foi projetada e construída. A comparação de dados simulados e experimentais mostrou que os tanques utilizados na plataforma experimental possuem perdas muito altas. Portanto, a plataforma experimental não conseguiu fornecer os resultados esperados para o experimento a longo prazo. A simulação, por outro lado, pôde ser validada através de testes específicos na bancada experimental. Logo, os resultados simulados representam o verdadeiro comportamento do sistema.

**Palavras-chave:** Aquecimento Solar para uso doméstico; Controle por informação meteorológica de meso escala; Validação experimental.



# Resumo Expandido

## 1.1 INTRODUÇÃO

O SWERA (Solar and Wind Energy Resource Assessment) afirma que uma das mais baixas irradiações globais anuais no território brasileiro está localizada na região de Florianópolis. No entanto, a radiação solar global anual nesta cidade é aproximadamente igual a encontrada em países como Espanha 55 % superior aos valores encontrados na Alemanha. Estes são países que já utilizam muito os sistemas de energia solar. Para piorar as coisas, chuveiros elétricos são amplamente utilizados no Brasil. Passos et al. relata que o uso de chuveiros elétricos no Brasil é responsável por 25 % do consumo total de energia doméstica e 70% das famílias brasileiras usam chuveiros elétricos.

Passos et al. também relata que o pico da demanda de energia causa problemas não só para o sistema de energia elétrica, que tem que reservar pelo menos 4 GW para fornecê-lo, mas também para a empresa de distribuição de energia elétrica devido à sobrecarga de cabo e / ou superdimensionamento e danos de transformadores. Pode-se pensar que um sistema de aquecimento de água doméstico solar padrão (SDWHS) poderia reduzir o consumo de energia nas horas de pico. No entanto, devido a tempo chuvoso, ou a uma sobrecarga no consumo de água quente, a quantidade de energia solar absorvida não seria suficiente, e um sistema de aquecimento de backup teria que ser fornecido, a saber, aquecedores de energia elétrica.

Analisando do ponto de vista da Primeira Lei da termodinâmica, o chuveiro elétrico é um conversor de energia perfeito. Ao analisar através da segunda Lei da termodinâmica, no entanto, este sistema de aquecimento possui uma eficiência de 3% a 4%. Portanto, destrói a capacidade de gerar trabalho. Um chuveiro elétrico é um dispositivo simples, mas não tem espaço para melhorias e a única maneira de evitar a perda de exergia é usar um processo termodinâmico diferente. Adicionalmente, o SDWHS padrão pode ser bom para o usuário, mas não resolve o inconveniente do pico da demanda de energia elétrica para a empresa de distribuição de energia. Portanto, um novo sistema foi proposto para transferir o consumo de energia elétrica para madrugada e aplanar o perfil de consumo de energia elétrica de uma casa. Este sistema usa dados de previsão do tempo para prever a energia solar absorvida pelo colector no dia seguinte, a fim de se preparar para possíveis condições climáticas desfavoráveis.

Estudos estão sendo conduzidos no LEPTEN (Laboratório de Engenharia de Conversão de Energia e Tecnologia de Energia) na UFSC, a fim de quantificar a possível redução de custos para a empresa de energia elétrica, desde que este seja usado massivamente pela população. As empresas de distribuição de energia elétrica poderiam reduzir os custos de produção e distribuição de energia no caso de o sistema proposto chegar ao mercado. Além disso, não seria necessário atualizar suas linhas de distribuição e usinas de energia com tanta frequência.

## 1.2 OBJETIVOS

O objetivo principal deste trabalho é apresentar simulação e um experimento em grande escala que foram realizados e construídos para transferir ou reduzir o pico de demanda de energia de uma habitação no Brasil. Neste trabalho, mostra-se uma análise mais detalhada dos efeitos dos erros de previsão do tempo. Também foi construído um experimento no intuito de validar a simulação TRNSYS para este sistema. Portanto, os objetivos deste trabalho são:

- Construir e obter dados de um experimento em escala real;
- Validar o modelo TRNSYS para este sistema;
- Aplicar o programa desenvolvido pela Koller e otimizado por Henrique Carminatti (2014) a outras cidades brasileiras e comparar os resultados;
- Estudar como os erros de previsão do tempo afetam o SDWHS proposto;
- Estudar como os erros de previsão do tempo afetam a operação e eficiência dos sistemas em diferentes cidades brasileiras;
- Estudar como a estratégia de controle de dias iguais aplicada pela Koller (2012) trabalha em outras cidades brasileiras. Nesse sentido, as principais contribuições deste trabalho são:
- Um maior detalhe na modelagem de tanques de armazenamento estratificados;
- A aplicação de experimento em Florianópolis para validar a simulação;

- A avaliação do efeito de diferentes métodos de previsão meteorológica no consumo diário de sistemas auxiliares de aquecimento;
- A análise do efeito das incertezas da previsão meteorológica na redução da demanda de energia elétrica no horário de pico;

### 1.3 METODOLOGIA

Um SDWHS usual é adequado para reduzir o consumo de energia de uma casa e, portanto, é um ótimo produto para reduzir os custos do usuário. No entanto esses sistemas não alteram o pico da demanda de energia. Colle et al. (2010) propuseram um sistema que é capaz de mudar esse pico de demanda de energia para madrugada e também reduzir os custos do usuário. Em vez de usar apenas um tanque de armazenamento, este sistema usa dois. Um tanque acoplado ao coletor solar. E o outro tanque, como um backup conectado ao tanque coletor, usando um dispositivo de pré-aquecimento. Tal sistema é denominado neste trabalho de SDWHS proposto, ou simplesmente PSDWHS. Pode-se imaginar que seria possível mudar o pico de demanda de energia por pré-aquecimento de água ao amanhecer usando um SDWHS padrão. No entanto, a eficiência do sistema depende da temperatura de entrada do coletor solar. O pré-aquecimento do tanque ao amanhecer diminui em grande parte a quantidade de energia absorvida pelo coletor solar. Essa é a razão por trás de usar dois tanques em vez de um. Com dois tanques é possível pré-aquecer a água ao amanhecer sem comprometer a capacidade de absorção de energia solar do sistema.

O PSDWHS foi simulado no TRNSYS (Um Programa de Simulação de Sistemas Transientes) e controlado com MATLAB. O programa foi projetado pela primeira vez por Koller (2012) e depois modificado por Carminatti (2014). A variável de controle é a temperatura de saída do tanque de backup, que nunca deve ser inferior a 39°C. O sistema foi simulado usando duas estratégias de controle diferentes. A primeira, proposta por Koller (2012), foi assumir que o dia atual será igual ao dia anterior. Portanto, os dados de radiação e temperatura do último dia são usados como entrada para calcular a quantidade de energia necessária para garantir o conforto do usuário. O outro método consiste em usar a previsão do tempo para prever a radiação total recebida pelo coletor do PSDWHS para o dia. Uma bancada de testes foi projetada e construída para obter dados experimentais para comparação e validação da simulação. Após este trabalho, a plataforma de teste permanecerá em operação para obter dados de longo prazo. Embora tenha havido



vários problemas com a funcionalidade do bancada de ensaio ao longo do tempo testado, foi possível usar os dados disponíveis para validar a simulação TRNSYS. Esta validação foi o objetivo principal de construir o a bancada. Uma vez que a simulação TRNSYS foi validada com dados experimentais, é possível utilizar esta simulação para calcular como o sistema se comportará em outras cidades, utilizando outras estratégias de controle ou usando diferentes previsão meteorológica simulada.

## 1.4 RESULTADOS E DISCUSSÕES

Na simulação há dois types principais que devem ser validados: O type 533, que corresponde ao tanque de backup; e o type 45a que corresponde ao tanque do coletor e aos coletores solares. Foi possível calcular a fração solar modificada dos sistemas para os dias de validação. Os valores para a radiação total incidente diária inclinada ( $G_t$ ), a energia auxiliar total ( $Q_{aux}$ ), a energia de carga total necessária ( $Q_{Shower}$ ) e a fração solar ( $MSF$ ) para 11 de junho e 22 de setembro são encontradas nas tabelas 2 e 1, respectivamente.

Conforme observado na tabela 1, valores de energia auxiliar total necessária são muito altos. Isto é devido ao fato de que a bancada de testes estava usando uma estratégia de pré-aquecimento fixa. Os valores para a fração solar para junho (tabela 2), em contraste, são muito melhores, no entanto, neste dia, o pré-aquecimento não foi necessário. Uma vez que estes são valores por um dia, estes não representam um comportamento mensal. Conforme mencionado anteriormente, a bancada de teste deve ainda ser submetida a um experimento de longo prazo para obter esses dados.

Outro resultado foram os gráficos das figuras 51, 52, 53, 54 e 55. Esses gráficos mostraram que à medida que os erros de previsão simulados aumentavam, o sistema não conseguiu fornecer água quente ao usuário com mais frequência. Este era um comportamento esperado. No entanto, esses gráficos foram construídos para buscar uma tendência que poderia justificar um ponto de parada para aumentar a precisão da previsão do tempo. No entanto, mais pesquisas devem ser feitas para rastrear esse ponto de parada.

## 1.5 CONSIDERAÇÕES FINAIS

O presente trabalho apresentou um projeto de sistema que foi capaz de transferir e encolher o pico de demanda de energia para água quente de uma casa, implementando um sistema de aquecimento de água doméstico controlado por previsão do tempo. Os objetivos apresentados neste trabalho foram alcançados e foi possível obter dados de uma bancada de testes e validar a simulação TRNSYS. Além disso, as simulações realizadas forneceram dados esperados e provaram que o sistema pode ser usado em muitas regiões brasileiras, transferindo o pico de demanda de energia de uma habitação. Conclui-se através das simulações que o sistema de controle poderia funcionar mesmo com informações meteorológicas não confiáveis, conseguindo transferir ou atenuar o pico de demanda de energia elétrica de uma residência. Isso garante uma grande contribuição para a empresa de distribuição de energia elétrica, uma vez que, se esse sistema fosse empregado em grande parte no Brasil, seria possível transferir ou encolher o pico de demanda de energia elétrica de toda a rede. Para a empresa de energia, isso significaria uma redução significativa de custos, uma vez que não seria mais necessário sobrecarregar a rede elétrica ou as usinas.

Uma bancada de testes do sistema foi construída e sua simulação pode ser validada. Para obter dados de longo prazo, o aparato experimental deve passar por algumas modificações. Primeiro, os seus tanques devem ser alterados ou modificados, pois os dispositivos instalados possuem um alto coeficiente de perda global ( $8\text{kw} / \text{hm}^2\text{K}$  e  $5\text{ kw} / \text{hm}^2\text{ K}$  para o tanque de backup e coletor, respectivamente). Em segundo lugar, os tubos do coletor devem ser verificados para procurar um bloqueio de fluxo de água, conforme observado através das diferenças de temperatura dos transdutores na figura 24. Esse bloqueio pode ser criado por material de solda ou fita de encanador em paredes de tubos. E, finalmente, deve-se alterar a placa de controle, ou seu programa, para aumentar a confiabilidade.

Os resultados apresentados indicam que o sistema poderia funcionar mesmo com informações meteorológicas pouco confiáveis. Mais pesquisas devem ser realizadas para acessar um melhor método para a previsão do tempo a ser usada na estratégia de pré-aquecimento. O leito de teste tem que, ainda, passar por um experimento de longo prazo para obter dados experimentais sobre fração solar e deslocamento de pico da demanda de energia elétrica



## ABSTRACT

Brazil uses many renewable energy sources. From hydropower, which is its main source, to the recent photovoltaic and wind farms. However, beneath the Brazilian energy resources is a negative truth: most dwellings in the country uses electric shower heaters. These devices are responsible for 43% of the Brazilian domestic electric energy demand peak. This peak causes problems not only to the electric energy system, which has to reserve at least four gigawatts to supply it, but also to electrical energy distribution company due to cable overload and/or oversizing and transformers damage.

In order to shift the electric energy use to dawn a novel Solar Domestic Water Heating system was simulated and tested. The objective of this system is to flatten the electrical energy consumption profile of a house. This system uses two tanks and weather forecast data to predict the solar energy absorbed by the collector for the next day in order to prevent for possible unfavorable climatic conditions. Computational analysis was carried using the TRNSYS software. Also a Test bed was built in order to compare results.

The presented system design was able to shift and shrink the energy demand peak for hot water of a household. Simulations delivered expected data and proved the system may be used in many Brazilian regions shifting the energy demand peak of a dwelling. However, as the simulated forecast errors increased, the system failed to deliver hot water to the user more often. More research must be done in order to trace down a tendency that could justify a stopping point on increasing the accuracy of the weather forecast. In addition, to validate the simulation the author designed and built a test-bed. Comparing simulated and experimental data showed that the tanks used on the experimental rig were far from ideal. Therefore, the experimental rig could not deliver expected results for the long-term experiment. The simulation, on the other hand, could be validated and its results represent the true system behavior.

**Keywords:** Solar domestic water heating system; System control using weather forecast information; Experimental validation.



## LISTA DE FIGURAS

|           |   |    |
|-----------|---|----|
| Figura 1  | Energy demand curve for two usual days, and for a day when the Brazilian soccer team was playing on the 2014 world cup (ONS, Date Accessed: 20/07/2017) ..... | 3  |
| Figura 2  | Configuration sheme of the PSDWHS.....  | 15 |
| Figura 3  | TRNSYS simulation analysis schematics.....  | 17 |
| Figura 4  | Hourly stochastic, daily stochastic and deterministic components of Solar Radiation.....  | 19 |
| Figura 5  | Graph of radiation values for the day 314 for the TMY, VTMY.....  | 20 |
| Figura 6  | Water load profile at 39°C used on the system simulation.....   | 21 |
| Figura 7  | Water consumption profile at 39°C for a household in England.....   | 22 |
| Figura 8  | View of the test bed.....   | 23 |
| Figura 9  | Test bed design scheme.....   | 24 |
| Figura 10 | Solar collector Jellyfish JF10.....   | 26 |
| Figura 11 | Solar collector Jellyfish JFS10.....  | 26 |
| Figura 12 | Open electronics box.....   | 27 |
| Figura 13 | Pyranometer installed on the test bed.....  | 28 |
| Figura 14 | SDWHS solenoid Valve.....   | 29 |
| Figura 15 | The Wired Arduino uno board of the test bed.....  | 30 |
| Figura 16 | The Wired Agilent 34972A data-logger of the test bed.....   | 31 |
| Figura 17 | Temperature transducers name and position.....  | 32 |
| Figura 18 | Temperature on the backup tank for the heat loss experiment on June 05.....   | 33 |
| Figura 19 | Backup tank validaton - Values for June 05.....   | 33 |
| Figura 20 | Backup tank out of sample validation - Values for June 15.....  | 34 |
| Figura 21 | Temperature on the Collector tank for the heat loss experiment on June 13 and 14.....   | 35 |
| Figura 22 | Collector Tank out of sample validation - Values for June 12 and 13.....  | 36 |
| Figura 23 | $G_t$ from experiment and $G_t$ from TRNSYS for June 15.....  | 37 |
| Figura 24 | Simulated and Experimental Collector temperature for  |    |

|  |    |
|--|----|
| June 15 .....  | 37 |
| Figura 25 Effective Area for June 15 .....   | 39 |
| Figura 26 Effective Area for January 19 .....  | 40 |
| Figura 27 Simulated and Experimental Collector temperature for<br>January 19 .....   | 40 |
| Figura 28 $G_t$ comparison for June 11 .....   | 41 |
| Figura 29 $G_t$ comparison for February 22 .....   | 41 |
| Figura 30 Collector Temperature for June 11 .....  | 42 |
| Figura 31 Collector Temperature for February 22 .....  | 42 |
| Figura 32 Collector Tank Temperature for June 11 .....   | 43 |
| Figura 33 Collector Tank Temperature for February 22 .....   | 43 |
| Figura 34 Backup Tank Temperature for June 11 .....  | 44 |
| Figura 35 Backup Tank Temperature for February 22 .....  | 44 |
| Figura 36 Auxiliary Energy consumption for every hour of the day.  | 48 |
| Figura 37 Year Average Auxiliary Energy Consumption for every<br>hour using asymmetrical square random distribution for the simu-<br>lation of weather forecast for Florianopolis. TMY-50% means that<br>forecasted radiation was 100% higher than real values. .... | 48 |
| Figura 38 Year Average Auxiliary energy consumption for every<br>hour using equal days strategy. Comparison between Florianopolis,<br>Sao Paulo, Brasilia, Santa Maria and Curitiba. ....  | 50 |
| Figura 39 A comparison of two different cities for number of 3 or<br>more consecutive dry day's period. ....   | 51 |
| Figura 40 Comparison between Florianopolis and Sao Paulo sunshine<br>hours. ....   | 51 |
| Figura 41 Energy Fraction Year Fraction graph for 10% simulated<br>weather forecast errors. ....   | 52 |
| Figura 42 Energy Fraction Year Fraction graph for 20% simulated<br>weather forecast errors. ....   | 53 |
| Figura 43 Energy Fraction Year Fraction graph for 30% simulated<br>weather forecast errors. ....   | 54 |
| Figura 44 Energy Fraction Year Fraction graph for 40% simulated<br>weather forecast errors. ....   | 55 |
| Figura 45 Energy Fraction Year Fraction graph for 50% simulated<br>weather forecast errors. ....   | 55 |
| Figura 46 Energy Fraction Year Fraction graph for Curitiba. ....   | 56 |
| Figura 47 Energy Fraction Year Fraction graph for Santa Maria. .   | 56 |

|   |    |
|---|----|
| Figura 48 Energy Fraction Year Fraction graph for Sao Paulo.....                            | 57 |
| Figura 49 Energy Fraction Year Fraction graph for Brasilia.....                             | 57 |
| Figura 50 Energy Fraction Year Fraction graph for Florianopolis..                           | 58 |
| Figura 51 Simulated forecast Errors Effect on Year fraction for 10%<br>Energy Fraction..... | 58 |
| Figura 52 Simulated forecast Errors Effect on Year fraction for 20%<br>Energy Fraction..... | 59 |
| Figura 53 Simulated forecast Errors Effect on Year fraction for 30%<br>Energy Fraction..... | 59 |
| Figura 54 Simulated forecast Errors Effect on Year fraction for 40%<br>Energy Fraction..... | 60 |
| Figura 55 Simulated forecast Errors Effect on Year fraction for 50%<br>Energy Fraction..... | 60 |
| Figura 56 Test bed Hydraulic Design.....  | 69 |
| Figura 57 Test bed Electric Design.....   | 73 |
| Figura 58 Test bed Electric Design.....   | 74 |
| Figura 59 Test bed control LABVIEW program.....   | 77 |
| Figura 60 Temperature and radiation data-logging.....                                       | 78 |
| Figura 61 Control Strategy.....   | 79 |
| Figura 62 System Clock.....   | 80 |
| Figura 63 Control procedure of the Arduino control board.....                               | 81 |





## LISTA DE TABELAS

|          |                                |    |
|----------|--------------------------------|----|
| Tabela 1 | Values for 22 of February..... | 46 |
| Tabela 2 | Values for 11 of June.....     | 46 |



## **LISTA DE ABREVIATURAS E SIGLAS**

- SDWHS - Solar Domestic Water Heating Systems
- PSDWHS - Proposed Solar Domestic Water Heating System
- TMY - Typical Meteorological Year
- VTMY - Varied Typical Meteorological Year
- CSR - Clear Sky Radiation
- SWERA - Solar and Wind Energy Resource Assessment
- LEPTEN - Laboratório de Eng. de Processos de Conversão e Tecnologia de Energia
- UFSC - Universidade Federal de Santa Catarina
- TRNSYS - Transient System Simulation program
- SMI - Swiss Meteorological Institute
- NIPS - National Integrated Power System



## LISTA DE SÍMBOLOS

- $S_{hor}$  - Hourly radiation value
- $S_{max}$  - Maximum radiation value for
- $E$  - Spencer's equation o time
- $S_t$  - solar time
- $R_t$  - Reference time
- $L_{hloc}$  - Local longitude
- $L_{ref}$  - Longitude used for the reference time
- $Q_s$  - Solar energy gain
- $Q_l$  - Heat load
- $Q_{Load}$  - Total heat load
- $Q_{losses}$  - Total energy losses
- $Q_{aux}$  - Total auxiliary energy
- $Q_{showerL}$  - Auxiliary energy used without the use of solar energy systems
- PT100 - Thermoresistance temperature transducer
- TCI - Lower collector tank PT100
- TCS - Upper collector tank PT100
- BTI - Lower Backup tank PT100
- BTS - Upper Backup tank PT100
- T+n - PT100 installed on the PSDWHS
- T-n - PT100 installed on the SDWHS
- JFS10 - Jellyfish selective surface solar collector
- JF10 - Jellyfish standard solar collector

- $SF$  - Solar fraction
- $M_{SF}$  - Modified solar fraction
- $m_{Load}$  - Mass to load
- $T_{Load}$  - Temperature at outlet
- $UA$  - Global heat loss coefficient
- $k_i$  - Insulation thermal conductivity
- $D_s$  - Insulation diameter
- $e_i$  - Insulation thickness
- $T_m$  - Average temperature
- $T_\infty$  - Ambient air temperature
- $T_{mix}$  - Mixture temperature
- $\dot{m}_{mix}$  - Mass flow rate at mixture
- $T_1$  - Temperature at collector 1 outlet
- $\dot{m}_1$  - Mass flow rate at collector 1 outlet
- $T_1$  - Temperature at collector 2 outlet
- $\dot{m}_1$  - Mass flow rate at collector 2 outlet
- $EA$  - Effective area
- $G_t$  - Solar irradiance at tilted surface
- $M$  - Mass
- $c$  - Specific heat of water
- $\Delta T$  - Temperature difference between  $39^\circ C$  and  $20^\circ C$
- WATSUN - Solar resource assessment software

## 1 INTRODUCTION

For most of human existence solar energy was only understood as light, being heat only a byproduct of it. For any solar energy system there are two basic ways to absorb irradiation: passively and actively. To position a building favored or not to sunlight, to use sunshades, paints or any material that favors or not the absorption of solar irradiation is to use passive solar energy engineering. Using photovoltaic panels or solar thermal energy absorber systems, on the other hand, is to use of active solar energy engineering. This last group is, as stated, divided in two great topics, photovoltaic and thermal solar energy. This work will cover some part of solar engineering of thermal process, more specifically the Solar Domestic Water Heating Systems aiming to reduce the electric energy load from shower heads in Brazil

The SWERA (Solar and Wind Energy Resource Assessment) states that one of the lowest annual global irradiation over the Brazilian territory is located in Florianopolis region. Nevertheless, the annual global solar radiation in this city is about the same value found in Spain(SANCHO et al., 2012) and 55% higher than values found in Germany(WIRTH, 2017). These are countries that already greatly use solar energy systems. To make matters worse, electric showers are extensively used in Brazil. Passos et al. reports that the use of electric showers in Brazil is responsible for 25% of the total domestic energy consumption(PASSOS, 2011) . Figure 1 shows the electric consumption profile in Brazil.

Figure 1 presents an energy demand for two regular days, and for a day when the Brazilian professional soccer team played on the 2014 world cup against Germany. It happens that when Brazil plays on the world cup employees are exempt from work. Since most people were already home, they did not shower during, or after, the game. Therefore, the curve shows a smaller energy demand peak because, as stated by Jannuzzi and Schipper (1991) up to 70% of the Brazilian households use electric showers.

Passos et al. also reports that the energy demand peak causes trouble not only to the electric energy system, which has to reserve at least 4 GW to supply it, but also to electric energy distribution company due to cable overload and/or oversizing and transformers damage(PASSOS, 2011). One could think that a standard solar domestic water Heating System (SDWHS) would be able to shrink the energy consumption at peak hours. Nonetheless, due to rainy weather, or an



overload on hot water consumption, the amount of solar energy absorbed would not be enough, and a backup heating system would have to be provided, namely electric energy heaters.

Analyzing from the First Law of thermodynamics point of view, the electric shower is a perfect energy converter. When analyzing through the second Law of thermodynamics, however, this heating system has an efficiency of 3% to 4%. Therefore, it destroys the capacity of generating work. An electric shower is a simple device, but, it has no space for improvement and the only way to avoid exergy loss is to use a different thermodynamic process.

Accordingly, the standard SDWHS may be good for the user but it does not solve the electric energy demand peak inconvenience for the energy distribution company. Therefore, a new system was proposed in order to shift the electric energy use to dawn and flatten the electric energy consumption profile of a house. This system uses weather forecast data to predict the solar energy absorbed by the collector for the next day in order to prevent for possible unfavorable climatic conditions.

Studies are being conducted at LEPTEN (Laboratory of Energy Conversion Engineering and Energy Technology at UFSC) in order to quantify the possible cost reduction for the electric energy company on the circumstance of this new system being massively used by the population. The electric energy distribution companies could reduce costs of energy production and distribution in the case the proposed system reach the market. Furthermore it would not be necessary to upgrade its distribution lines and power plants so often.

The main goal of this work is to present simulation and a full scale experiment that were carried out and built in order to shift or reduce the energy demand peak of a dwelling in Brazil. In this respect, some contributions are studied to be added to the works of Salazar (SALAZAR, 2004), Passos et al. (PASSOS, 2011), Koller (KOLLER, 2012) and Carminatti (CARMINATTI, 2014). In this work a more detailed analysis of the effects of the weather forecast errors is shown. Also a full scale experiment was built in order to validate the TRNSYS simulation for this system. Therefore, the goals of this work are:

- To build and obtain data from a full scale experiment;
- To validate the TRNSYS model for this system;
- To apply the program developed by Koller and optimized by Henrique Carminatti (2014) to other Brazilian cities and compare results;

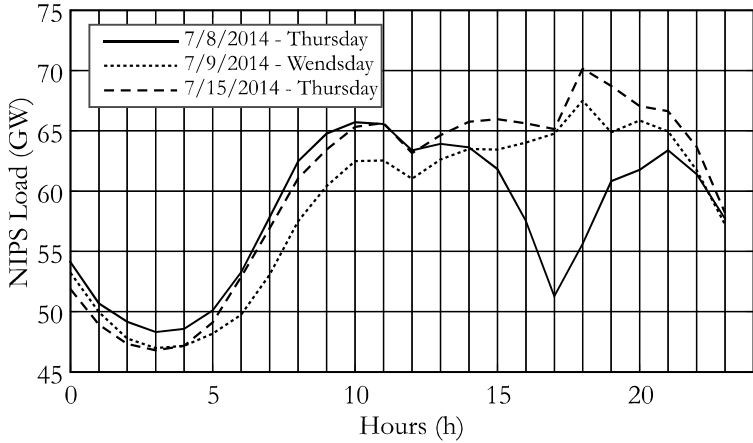


Figure 1 – Energy demand curve for two usual days, and for a day when the Brazilian soccer team was playing on the 2014 world cup (ONS, Date Accessed: 20/07/2017)

- To study how the weather forecast errors affect the proposed SDWHS;
- To study how the Weather forecast errors affect the systems operation and efficiency in different Brazilian cities;
- To study how the equal days control strategy applied by Koller (2012) works on other Brazilian cities.

In this sense, the main contributions of this work are:

- A greater detail in the modeling of stratified storage tanks;
- The application of a full scale experiment in Florianopolis to validate the simulation;
- The Assessment of the effect of different forecast methods in the prediction of everyday consumption of auxiliary heating systems, and;
- The analysis of the effect of forecast uncertainties in the reduction of electric energy demand at peak hours;

Therefore, the present dissertation is going to be divided as follows: first, on chapter 2, there will be a literature review of this dissertation's scope and the basic theory of some solar energy topics. Then, on chapter 3 will present the proposed SDWHS, its control strategies used and simulated on this work, and the computational method alongside its main variables. The full scale experiment will be shown on chapter 4, the test rig was built on top of the Solar Energy Laboratory at UFSC, Its data and the simulation validation will also be presented on this chapter. Chapter 5 will list the results of the simulations. Chapter 6 will hold this work's conclusions and future works.

## 2 BACKGROUND AND LITERATURE REVIEW

Solar collectors are a special type of heat exchangers. Differently from common types that exchange heat between two fluids, the solar collectors obtain energy from the solar radiation and transfer it to a work fluid, usually water.

The flat plate collector is a basic type of solar collector. These collectors do not need a sun tracking device because it works using both diffuse radiation and direct radiation. Usually, these collectors are installed on rooftops, facing the equator. On the south hemisphere the collector should be facing north and in the case of Florianopolis should be inclined by  $37^\circ$ . This inclination value corresponds for the city latitude plus  $10^\circ$ . This is suggested by Duffie and Beckman (2006) to favor the solar radiation on winter, when the sun is closer to the horizon.

### 2.1 SOLAR SYSTEMS SIMULATION AND DATA SERIES

To study and simulate a solar energy system a data series from the location of interest must be used. Differently from other engineering systems, solar energy systems are highly dependents on location's weather. One way to overcome the difficulty of simulating such system is using a TMY (Typical Meteorological Year) for the region of interest.

A TMY is constructed to "correspond to an 'average' year regarding both the occurrence and persistence of warm/cold, sunny/overcast and/or dry/wet periods in all months or seasons" (FESTA; RATTO, 1993). There are many different methods to select such months, but the most used is the Sandia Laboratories method (SKEIKER, 2007). Using this methodology the TMY is formed by selecting months over a 30 year hourly data set. TMY is, therefore, a year formed by months representing a median regarding selected meteorological variables. In the case of not having such a long data series available other methodologies may be used to overcome this difficulty. For this Dissertation the TMYs for the selected cities were obtained from the Solar and Wind Energy Resource Assessment (SWERA, 2001) database.

In order to simulate this work's proposed solar domestic water heating system (PSDWHS) a TMY and another data series representing the weather forecast had to be used. This weather forecast simulator is a varied TMY that maintains the same properties of the original

series. To build such VTMY the following Boland articles were taken into consideration.

### **2.1.1 Climatic Variables and simulated Weather Forecast Errors**

In 1995 Boland showed a procedure on building synthetic series of climatic variables which have the same statistical properties as real time series. Even though the rigorous approach presented in this article was not used in this dissertation, its idea was used to create the varied TMY that was used to simulate weather forecast.

While Boland (1995) uses a Fourier transformation in order to get rid of the hour-to-hour and keep the day-to-day stochastic component of the solar radiation, in this dissertation, the author aims to keep the hourly, and change the daily stochastic component by multiplying it by a random factor. The simulated weather forecast error is created this way. This article has its importance here, since it is able to show that these synthetic series of climatic variables have the same statistical properties of the real time series for the same locations.

More importantly, in the subsequent publication, Boland (1997) investigates the need of including the stochastic component of weather variables in simulation studies of the thermal performance of houses. Even though the thermal performance of houses is not the scope of this dissertation, it presents that the daily total radiation residuals can be represented by a first order autoregressive process. He also states that these results can be used to construct a synthetic sequence for radiation data. This can be used on future works to improve this dissertation's simulated weather forecast errors.

The author also describes that: "It is conjectured that if there is a significant cross-correlation between the variables in the original time series it resides primarily in the deterministic component"(BOLAND, 1997). Which means that one does not need to create a variation on the temperature as its stochastic component is assumed to not have a correlation with the solar radiation. This is plausible because the stochastic component of the radiation has greater relation to instantaneous cloud cover than with ambient temperature. This happens due to the fact that the ambient air has a considerable thermal capacity when pondering the time period of a cloud blocking the direct sun light.

Thus, the author concludes that the stochastic day-to-day components of the temperature and radiation must be considered (BOLAND,

1997). However, referring to Hollands, D'Andrea and Morrison (1989) work, Boland (1997) states that for process heat systems it would seem necessary to be able to construct synthetic sequences for radiation only. This means that for this case the temperature day-to-day stochastic component can be neglected.

### 2.1.1.1 Synthetic Data-sets

Boland and Dik (2001) improved Boland's previous strategy on creating synthetic series. In this case, a simulation to investigate whether or not the hour-to-hour stochastic component of solar radiation was considered and mathematical testing of performance of models of various systems utilizing solar energy was held.

The investigation consisted on a large number of simulation using two different types of data-sets, this simulation was carried out on WATSUN program. One type consists of measured hourly radiation data, therefore including stochastic and deterministic components; and another, included hourly values determined from smoothing this data on daily basis, thus including only deterministic component.

To create the smoothed data file, Boland and Dik (2001), used the previously mentioned Fourier transformation on the hourly data over a day. The spectrum of amplitudes was examined and concluded that the use of 3 harmonics was sufficient to model the diurnal variations. The investigation included the effects of hourly stochastic component in 3 different systems: a standard SDWHS, a photovoltaic system, and house thermal performance system.

For all cases, for the hypothesis to be supported, both selected statistical criteria were found to be satisfied:

- the results for two data-sets were statistically indistinguishable;
- and the tests supported the concept that the two methods yields the same variance in measurement. In this case it was considered that each simulation with different data set is a different measurement method. Which means that the theory of measurement is supported.

The authors concluded that for domestic solar water heaters, there is no statistically significant difference in the results, from simulation software, whether or not the hour-to-hour stochastic component of solar radiation is included in the input data set (BOLAND; DIK, 2001). This complements the results from both previous Boland's arti-

cles (1995 and 1997). Therefore, the day-to-day stochastic component is required to properly simulate the SDWHS, while the hour-to-hour stochastic component of solar radiation is not. However, the simulated and tested SDWHS did not have an intelligent control strategy for the auxiliary heater, and did not use weather forecast data. Therefore, it is possible that the stochastic component of the hour-to-hour solar radiation could have a significant interference on the results of such system.

## 2.2 WEATHER FORECAST CONTROLLED SOLAR ENERGY SYSTEMS

The oldest work found on using weather forecast to control a SDWHS is from Grünenfelder and Tödtli (1985). On this article a standard SDWHS with an electric auxiliary heater is studied. The authors compared six different control strategies for this system as follows:

- To use the meteorological forecast from the official SMI (Swiss Meteorological Institute).
- To apply a predictive control that copies the last day data as input data for the next day. This is, in fact, the equal days strategy used in this dissertation, but the authors employed it to not only to weather forecast but also to the hot water consumption and heat losses.
- To use one of 4 previously set auxiliary heater control setups based on a data series from 1963 to 1972 for the next day predicting in this fashion, the next day's solar energy gain.
- To use energy price forecast for the next day and the energy absorbed in the collector on the present day to obtain a control strategy for the auxiliary heating for the following day;
- To use a dynamic programming algorithm for the next day auxiliary heating.
- To use a fixed control strategy that was calculated based on a meteorological data series, from 1963 to 1972.

The authors concluded that the systems performance depends on the tank volume. However, considering all simulated cases, the ones using meteorological data and weather forecast obtained the best results. Thus, the importance of researching on this topic is revealed.

### 2.2.0.1 Weather and Load Forecast

Prud'homme and Gillet (2001) studied the possibility of using not only weather forecast to establish a control strategy for the auxiliary heater but also tries to develop a predictive control of the user's hot water consumption. To do so, the authors used a closed loop SDWHS with a highly stratified vertical tank. This means that there is a heat exchanger inside the boiler. This is common in cold weather areas. In order to prevent freezing on the collector tubes, they are filled with antifreeze fluids in a closed loop configuration. The auxiliary heater is segmented to enable the great stratification of the tank.

The tank temperature control is based on minimizing a function for each day's electrical energy consumption and user comfort. In such a function, however, the different energy prices between day and night are not taken into account. To consider the energy consumption, the authors, used meteorological data from the Swiss Meteorological Institute (SMI) for the next two days. Whereas, to predict the consumption profile, an average of the hot water load is made from the same days of the week for the last two months and a Kalman filter is applied to obtain future consumption values.

There were two different simulations, one daily and another for 28 days. As a result the authors state that, using the suggested control approach, it is not necessary to keep the auxiliary heaters continuously on, but rather to an on/off system. Thus the auxiliary heating is only powered just before that hour's hot water consumption. Therefore, it is possible to keep the reservoir at a lower temperature during the day, reducing the thermal loss. This fact, according to the authors, was the main element to increase the solar fraction in the system. The authors emphasize that the results were simulation and non-experimental, concluding that more studies should be done to guarantee the efficiency of the system.

When there is no other bindings rather than just the operations costs and the solar fraction the best control strategy is to preheat the tank closer as possible to the user consumption to avoid thermal losses. However when brought to Brazilian, and to this dissertation reality, this control strategy is not ideal since it does not consider energy costs or the energy demand peak.

The implemented Kalman filter could always identify the user load profile. To implement the method explained on the article for load prediction in a future commercial product based on this dissertation may be a good idea, in order to establish the users hot water load



profile.

Finally, the authors explain that for commercial use it may be difficult to obtain the weather forecast for each SDWHS separately. In addition, this control strategy demands a complex optimization and significant computational capacity (PRUD'HOMME; GILLET, 2001). This, however, may not be the reality anymore due to newer control boards and cloud computing services.

### 2.2.0.2 Modern Weather and Load forecast Strategy

Vivaudou (2014) used a standard SDWHS using weather and load forecast. For the weather forecast the author uses a 5 year radiation data set to establish a maximum radiation value for each month. The author obtains from the Internet the predicted cloud cover for the next day and compares it with the 5 year data set. If cloud cover is 0%, the maximum amount of radiation found in the data set for that month is selected. Equation 2.1 shows the used function to obtain the radiation forecast based on cloud cover.

$$Shor = Smax * (1 - CloudCover). \quad (2.1)$$

The author used 3 different setups to control the auxiliary heating system depending on the cloud cover forecast: Sunny day, partially sunny, or cloudy. For each of these conditions a fixed amount of energy was delivered to the tank. The weather forecast used has not been compared to other real forecasting and has not been compared to real data to access its efficiency. The model was programmed in excel and lacks accuracy or modeling deepness. The author concludes that the weather forecast can be beneficial to the control decision and strategy of SDWHS.

Although Vivaudou does not deepens the study, it is noteworthy to present this work here in order to emphasize the international curiosity on weather forecast controlled solar domestic water heating systems and, therefore, the importance of the present dissertation.

### 2.2.1 Starting point of the PSDWHS

Salazar (2004) established a methodology for the potential savings and reducing of the electric energy demand curve at peak hours for low income consumers through the use of compact solar heating

systems. He also validated the computational model of the solar collector of the TRNSYS software. At last he could economically optimize the constructive parameters using multi-objective programming for a group of consumers with varied hot water consumption profiles.

Salazar, also made a four month in site research, from February to may 2004, where he accessed information about the low income families hot water consumption, its impact on the SDWHS and over the electric energy load. This research allowed for the creation of a hot water consumption profile implemented in Koller 2012, Carminatti 2014 and in this dissertation's computational analysis.

### **2.2.2 Design of the PSDWHS**

The conventional solar heater, proposed as a solution for Brazil to completely dissociate or reduce the electric showers based peak load, is not an effective solution (COLLE et al., 2010). The electric shower power load profile remains virtually unchanged when unfavorable climatic cycles are repeated. Thus, Colle et al. (2010) proposed a solar heating system with an intelligent auxiliary heater control strategy and a two tanks design. In this system, the hot water is preheated at dawn, when the electric energy tariff would reach its minimum, in the circumstance of an effectively regulated energy market. The two tanks design is important since the collector's efficiency is driven by its inlet water temperature. Therefore, preheating the collector tank at dawn would have a great negative effect on energy absorbed by the collector, increasing the auxiliary energy consumed. Since the preheating the tank at dawn would largely increase the daily energy losses by the system's tanks, these authors, also addressed the optimization of the thermal insulation of reservoirs, for different conceptions and modes of operation of the solar heating system.

### **2.2.3 System effectiveness measurement**

Duffie and Beckman (2006) define the measure of the systems effectiveness as the ratio of two similar quantities: the solar energy gain and the electric energy load that would be needed on a zero area solar energy system. This ratio is called Solar Fraction, and it represents the amount of energy that could be saved for a day, a month or a year

when using the SDWHS. On equation 2.2 is the defined function.

$$S_F = \frac{Q_s}{Q_l} \quad (2.2)$$

Where " $S_F$ " is the solar fraction,  $Q_s$  is the solar energy gain and the  $Q_l$  is the heat load.

This equation does not account for the parasitic energy use of the system, for instance, the energy needed to run a pump, or to control the whole system. The solar energy system used and explained in this dissertation does not have an integrated pump, then, it works as a thermosiphon. In addition, the energy used to control the system is way less than the auxiliary heat input, therefore, one can disregard such energy use.

### 2.2.3.1 Simulation of the PSDWHS: Equal Days Strategy for Florianópolis

Koller (2012) simulated the system previously conceived by Colle et al. (2010), implementing an algorithm on TRNSYS software. It presented a control strategy for the backup tank preheating device without the need of meteorological forecast directly. Such control used only the data obtained from the reservoir, the user hot water consumption and solar radiation from the previous day as input data for the present day preheating control strategy. The idea behind this control strategy was to build a cheap system for low income dwellings that could shift and shrink the house's electric energy demand peak. As a result, it obtained a solar fraction of 64.69% for Florianópolis. In addition, it analyzed the electric energy peak reduction comparing it to a standard solar heating system (without the backup tank). The proposed system could reduce the electric energy peak in 99.8% for a low income household, while a standard system could reduce 85.4%.

### 2.2.3.2 Simulation of the PSDWHS: Simulated Weather Forecast Errors for Florianópolis

Carminatti (2014) continued the study of the double tank system configuration initiated by Koller (2012). The author modified Koller's algorithm on TRNSYS software in order to obtain higher simulation speed. By doing so the author changed the simulated control system

to calculate, not a set temperature, but rather an amount of energy to be delivered to the backup tank for the day.

In addition, it conducted simulations on the effects of simulated weather forecast errors on the proposed system for Florianopolis. In this sense, it used a noise generator to modify the predicted values of incident solar radiation. For an ideal system, namely without errors in the weather forecast, the author obtained a solar fraction of 87%. While for the worst simulated case, with a simulated weather forecast overestimating solar radiation up to 100%, the solar fraction of the system was about 75%. In this case 57% of the household's electricity demand could be shifted to dawn, between 4 am and 6 am, far from the peak hours from 6 p.m. to 9 p.m.

The present work aims to continue Salazar (2004), Colle et al. (2010), Koller (2012), and Carminatti (2014) works by applying the above mentioned TRNSYS simulation to other 4 Brazilian cities. A full scale of the proposed system was also built on the rooftop of LEPTEN at Federal University of Santa Catarina in Florianopolis.



### 3 SDWHS AND SIMULATION

A usual SDWHS is well suited to reduce the energy consumption of a house and therefore it's a great product to cut down the user's costs. However, as stated before, these systems do not shift the energy demand peak. Colle et al. (2010) proposed a system that is capable of shifting this energy demand peak to dawn and also reduce user's costs. Instead of using only one storage tank, this system uses two. One tank coupled to the solar collector. And the other tank, as a backup connected to the collector tank, using a pre-heating device. Figure 2 shows the schematics of this system from now on called Proposed Solar Domestic Water Heating System, or just PSDWHS.

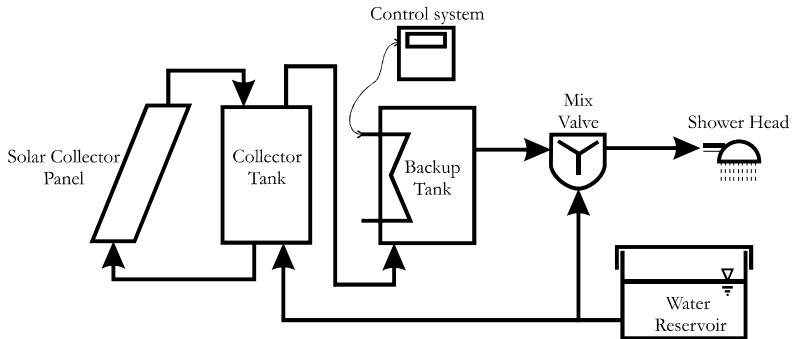


Figure 2 – Configuration scheme of the PSDWHS.

One can imagine that would be possible to shift the energy demand peak by pre-heating water at dawn using a standard SDWHS. However, the solar collector inlet temperature drives the system's efficiency. Pre-heating the tank at dawn would largely decrease the amount of energy absorbed by the solar collector. That is the reason behind using two tanks instead of one. With two tanks it is possible to pre-heat water at dawn without compromising the system's solar energy absorption capability.

### 3.1 COMPUTATIONAL ANALYSIS

The PSDWHS was simulated on TRNSYS (A Transient Systems Simulation Program) and controlled with MATLAB. The program was first designed by Koller (2012) and then modified by Carminatti (2014). The control variable is the backup tank outlet temperature, which should never be less than 39°C, therefore the auxiliary heat input of the backup tank is controlled.

TRNSYS is a complete and extensible simulation environment for the transient simulation of thermal systems (KLEIN et al., 2010). It is used to validate new energy concepts, from simple solar domestic hot water systems to the design and simulation of buildings and their equipment, including control strategies, occupant behaviour, alternative energy systems (wind, solar, photovoltaic, hydrogen systems), etc. This program uses pre-programmed subsystems blocks, called "Types", which the user unites to create complex systems and its inputs and outputs of heat, mass, information.

The simulation used the Type 45-a to model the solar collector and the collector tank altogether. This Type models a thermosyphon system consisting of a flat plate collector and a stratified storage tank. This tank may be vertical or horizontal on the model, but, in order to build a compact system a horizontal tank was selected. Flow in the loop is assumed to be steady-state. The system is analyzed by dividing the thermosyphon loop into a number of segments normal to the flow direction and applying Bernoulli's equation for incompressible flow to each segment (KLEIN et al., 2010). The flow rate is obtained by numerical solution of the resulting set of equations. On this configuration a time step of 1 hour is sufficient.

The proposed system is controlled by inserting information of the auxiliary heating device on Type 533. This component models a cylindrical tank on a horizontal configuration. The fluid in the storage tank interacts with the environment (through thermal losses from the left end, right end and top and bottom edges) and with up to two flow streams that pass into and out of the storage tank. The tank is divided into isothermal and isochoric nodes (to model stratification observed in storage tanks) where the user controls the degree of stratification through the specification of the number of "nodes" (KLEIN et al., 2010).

Although the tank has only 70 liters and is placed horizontally a five node configuration was selected for the simulation. Each constant-volume node is assumed to be isothermal and interacts thermally with the nodes above and below through several mechanisms: fluid con-

duction between nodes, and through fluid movement. Auxiliary heat may be provided to each isothermal node individually through the use of miscellaneous heat inputs to the model. The model also considers temperature-dependent fluid properties. Figure 3 shows the main fragment of the systems simulation on the TRNSYS software.

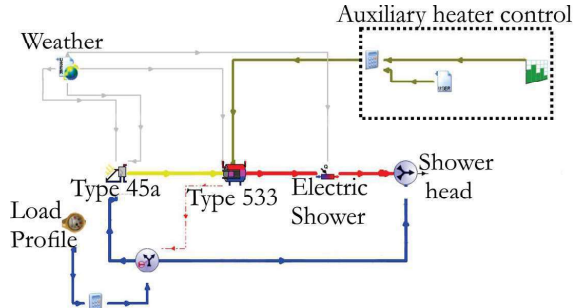


Figure 3 – TRNSYS simulation analysis schematics.

If one could perfectly predict not only the weather but also the user's hot water load an electric shower as shown on figure 3 would not be needed. To use this electric shower seem contradictory since one is trying to avoid using electric energy at peak hours, however, on real situations an electric passage heater must be added to the system to guarantee user comfort.

### 3.2 THE PROPOSED CONTROL STRATEGIES AND SIMULATED WEATHER FORECAST ERRORS

The system was simulated using two different control strategies. The first one, proposed by Koller (2012), was to assume that the present day is going to be equal as the previous day. Therefore, last day's radiation and temperature data are used as input to calculate the amount of energy needed to guarantee user comfort. The other method consisted in actually using weather forecast to predict the total radiation received by the collector of the PSDWHS for the day. This work's scope does not include showing the details of a real control strategy using weather forecast for a solar domestic hot water system, only its simulation.

The test bed built as part of this work did not use a real forecast control strategy too. The test bed was used to validate the TRNSYS



simulation in this work. Therefore, it could not use the TRNSYS program alongside a weather forecast because it was not validated yet. However, a simple approach to implement the weather forecast control strategy would be to use the laboratory's weather forecast data and this simulation on TRNSYS. At every morning a computer would run the TRNSYS program in order to predict the system's behaviour and calculate the preheating energy. But, as stated before, this was not done. The auxiliary heating control strategy implemented on the test bed used a fixed amount of preheating energy. This was much easier to implement and served perfectly for the test bed purpose in this work.

### **3.2.1 Simulation Control Strategy 1: Equal Days**

It is reasonable to ponder that weather does not change quickly. Of course sometimes the weather does changes from one day to another, but generally speaking, it does not. One can take the 20 consecutive rainy days that happened from March to May this year (2017) as an example. In this case the equal days strategy would only miss on two days: the first day and after the last. As stated before, this control strategy was designed for cheap systems to be used on low income dwellings. Therefore, the lack of connection to the internet and a simpler control device are important in order to shrink product costs. Koller applied this control strategy to his simulation and obtained solar fraction of 66% on the PSDWHS for Florianopolis, but it is worth mentioning that Carminatti has modified the TRNSYS simulation program designed by Koller in order to have better computational efficiency.

### **3.2.2 Simulation Control Strategy 2: Weather Forecast**

As explained before, to study and simulate a solar energy system a TMY from the location of interest must be used. In this case, because one is trying to simulate a system using weather forecast information another TMY must be used in order to emulate such forecast. Therefore the solar radiation variables of the Typical Meteorological Year (TMY) were varied using a noise generator to emulate the weather prediction and its errors. For each simulation two TMYs were used. One representing the real weather during the year, and another representing the weather forecast.

Inman et al. (2014) states that, variability of solar irradiance

at ground level is most affected by solar position and cloud cover, the latter influence is stochastic and difficult to model or predict. Boland, however implies that the stochastic component of solar radiation variables can also be broken down on to two other component: daily and hourly components. Therefore, Boland (1995) uses a Fourier transformation in order to get rid of the hour-to-hour and keep the day-to-day stochastic component of the solar radiation. By doing so Boland simplifies his synthetic series and Boland (1995) also states that the hourly stochastic component is not important for solar thermal engineering calculations. However, for this work, the hourly component - or, in other words, the cloud cover influence - of the solar radiation was kept in the data series. All of Boland's simulations (1995, 1997 and 2001) only regarded standard SDWHS, without the usage of weather forecast or a backup tank. Therefore, in this dissertation, the author aims to keep the hourly and changed only the daily stochastic component by multiplying it by a random factor. Figure 4 explains the difference between these components of the solar radiation, and figure 5 shows the difference between the VTMY and TMY for a selected day of the year.

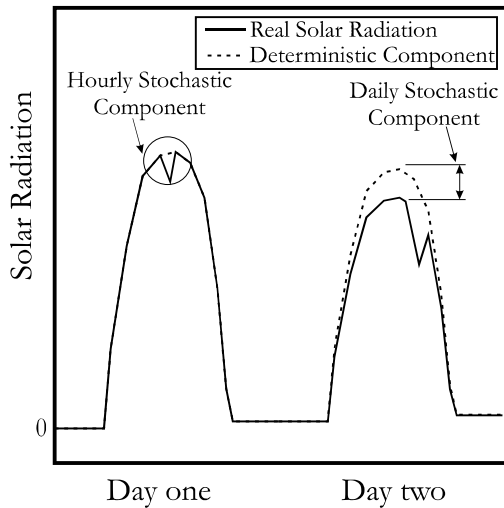


Figure 4 – Hourly stochastic, daily stochastic and deterministic components of Solar Radiation.

The applied noise on solar radiation values has a square random distribution that it applied to each day of the year, pushing the solar radiation graphic down. As stated before only the daily stochastic component of the radiation is modified. The profile of the random distribution is arbitrary and, it probably does not represent reality. However, the objective is not to simulate the weather forecast's errors or its residuals in its perfection, but to only analyze the effects of weather prediction errors on the SDWHS. Therefore, five new TMYs were created using asymmetrical square random distributions called VTMYs (varied typical meteorological years) in order to always over predict the solar radiation. For future works it may be interesting to analyze the distribution of weather forecast error.

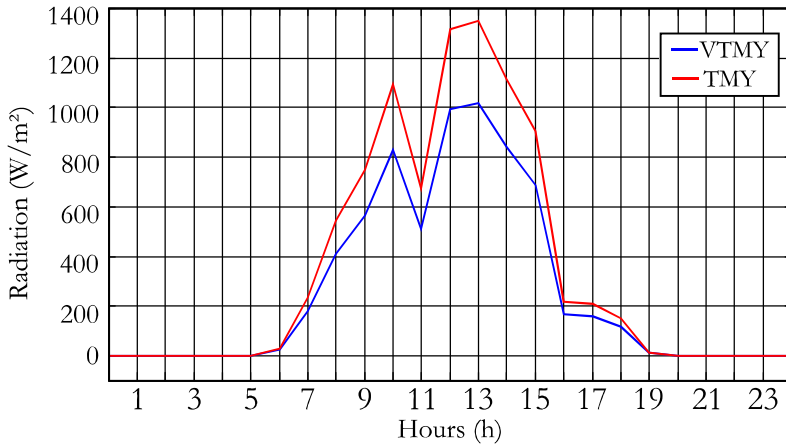


Figure 5 – Graph of radiation values for the day 314 for the TMY, VTMY.

The only variable altered on the VTMY was the solar radiation. This was done because "the day-to-day stochastic temperature component was not required when evaluating the performance of solar process heat systems (HOLLANDS; D'ANDREA; MORRISON, 1989). Therefore, it was not necessary to simulate the weather forecast errors of such climatic variable.

### 3.2.3 Load Profile

Besides the above-mentioned input data, water output load profile must be selected to simulate the hot water consumption in a house. It is well known that domestic hot-water use varies day by day, hour by hour, and minute by minute. For use in simulations the average load must be distributed over days and hours(DUFFIE; BECKMAN, 2006). Salazar (2002)(SALAZAR, 2004) studied water consumption profile on Brazilian low income households and reached the profile presented as a graph on figure 6. This consumption profile, however, is based on few months, therefore it's use must be cautious.

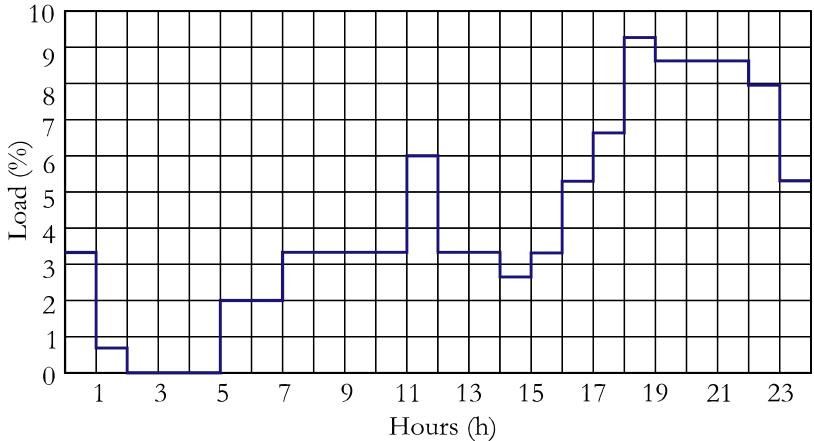


Figura 6 – Water load profile at  $39^{\circ}\text{C}$  used on the system simulation.

Passos (2011), Koller (2012), Goncalves (2014) and Carminatti (2014) used 200 liters of hot water a day for a house, therefore this work also used the same value for the total amount of hot water consumed in a dwelling.

For comparison purposes, Vivaudou (2014)(VIVAUDOU, 2014) was also able to obtain a hot water consumption profile, but for a district in England. On figure 7 is such load profile.

The difference between these two load profiles are clear. While the Brazilian low income profile has a more spread hot water usage, the English hot water use is mainly happening in the morning. It is inverted when the water load peak hours are compared. The Brazilian has peak hours, from 5pm to 10pm while the English has its water consumption

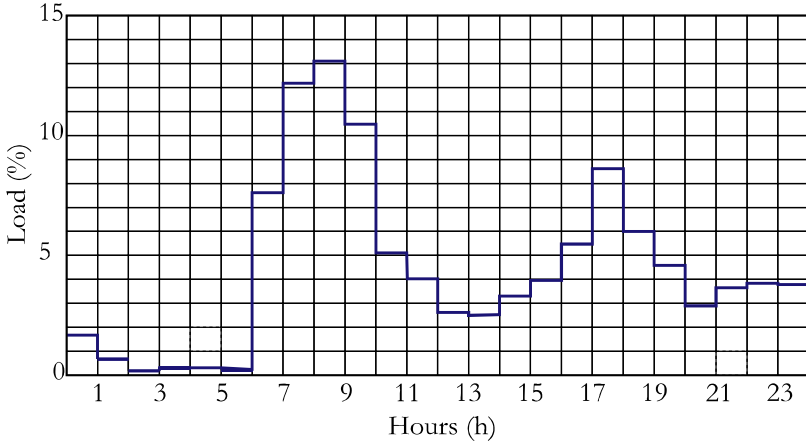


Figure 7 – Water consumption profile at  $39^{\circ}\text{C}$  for a household in England.

peak from 6am to 10am. Both these hot water loads have its trade-offs. Whilst, the Brazilian load profile happens during electric energy peak hours compromising the electric energy distribution sector. The English one happens during the morning, when there was not enough time yet for the solar energy systems to properly operate.

## 4 FULL SCALE EXPERIMENT

A test bed was designed and built in order to obtain experimental data for comparison and validation of the simulation and its results. This test bed is capable to obtain data from two different systems, at the same time, using the same control strategy. Both, a PSDWHS and a SDWHS are being tested at the rooftop of the Laboratory of Energy Conversion Engineering and Energy Technology (LEPTEN) at UFSC for future comparison of these systems. Also, after this work the test rig will remain on operation in order to obtain long term data. Figure 8 shows the outside rig of the experimental apparatus, on the left side of the picture is the PSDWHS and on the right side, the SDWHS. Appendixes A and B present the hydraulic design and the electric wiring of the system.



Figura 8 – View of the test bed.

### 4.1 TEST BED APPARATUS

The test bed design and its main components are going to be explained on the next sections, most of these components can be found on figure 9.

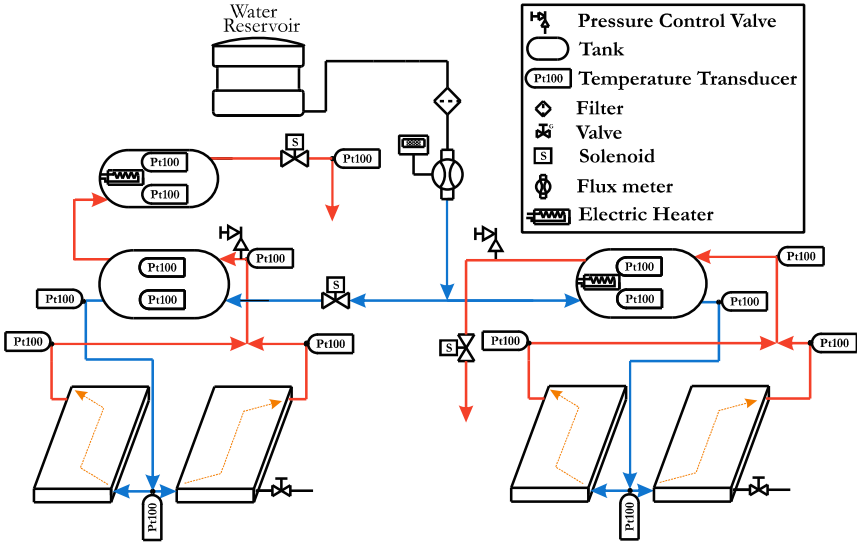


Figura 9 – Test bed design scheme

### 4.1.1 Structure and Basic Devices

The structures are made of, mainly, 4 millimeters thick Stainless steel trims, only the tubes and connections being made of copper or brass. The structure was designed by Koller (2012). It is a heavy structure to avoid damages caused by wind gusts, common in winter in Florianopolis.

#### 4.1.1.1 Tanks

There are three tanks installed on the test bed. Two for the PSDWHS and one for the SDWHS. These tanks were already available at the laboratory and have different insulation thickness.

The PSDWHS has a tank for the collector loop, called from now on Collector Tank, with 130 liters and no auxiliary heating device. This system also has a backup tank of 70 liters where the auxiliary heater is installed. The collector tank and the backup tank have 10 cm of insulation thickness. As explained on chapter 2, the second tank

is used to heat the water at dawn without compromising the systems solar energy absorption capabilities in order to shift the user's energy consumption away from the Brazilian energy demand peak.

The SDWHS has one tank with capacity for 200 liters and insulation thickness of 5 cm.

It is worth noting that the tanks used in this test bed were already available at the laboratory and were not selected by this dissertation's author. The SDWHS tank, specially, was bought in 2007 for another project, and thus, does not have a global loss coefficient equal to the others PSDWHS tanks. In addition, during validation process the tanks were found to have a high global loss coefficient. This affected experimental data as the test rig could not deliver the expected behaviour. However, the obtained experimental data is still worth for the simulation validation since it is possible to change the tank's properties on the program.

#### 4.1.1.2 Auxiliary Heaters

While the backup tank of the PSDWHS has a 1.5 kW auxiliary heater, the SDWHS tank has a 3 kW device. Although these heater were already installed on the tanks it is not inadequate to have a smaller heater on the smaller tank. However, it is necessary to feed both systems with the same amount of energy, thus, the PSDWHS heater has to be turned on for twice as long as the SDWHS.

#### 4.1.1.3 Collectors

There are 4 collector installed on the test bed. However they are not the same model. There are two Jellyfish JF10, as seen on figure 10, and two Jellyfish JFS10, as seen on figure 11. These Solar Collectors were a donation to the project. One of each type has been installed on each system, therefore, both systems have the same solar collector parameters.

#### 4.1.1.4 Water Filter

A water Filter was installed on the system in order to prevent clogging specially on the solar collector. It is a security measure since this is a long term experiment.





Figura 10 – Solar collector Jellyfish JF10.



Figura 11 – Solar collector Jellyfish JFS10.

#### 4.1.1.5 Pull and Outside Electronics Boxes

There are 2 pull boxes and one electronics box on the test bed. These boxes were installed for easy access and maintenance of the test bed wiring. The electronics box shown on figure 12, however, was installed as a shelter for the Solid State Relays, safety fuses, wiring connections and other electronic devices, it is also where the test bed is powered.



Figura 12 – Open electronics box.

## 4.1.2 Measurement Equipments

In the test bed many measurements components that are not going to be necessary in the final product were installed. However these components are useful to determine, for example, the heat loss on the tubes to validate simulation results.

### 4.1.2.1 Temperature Transducers

In order to obtain temperature data from the test bed, 16 PT100, platinum resistance thermometers, were installed. Seven on the SDWHS and nine on the PSDWHS. There are two PT100 on each PSDWHS tanks to account for temperature differences and heat loss. One transducer in the outlet pipes for each system to log the outlet water temperature. And all the others are on the tubes to account for heat loss. On a future product, only two temperature transducer would be necessary, one to obtain the inlet water temperature and another for the tank outlet temperature. It is worth noting that all of the temperature transducers are wired to the Agilent data-logger.

These PT100 temperature transducers, were factory calibrated. However, some of the PT100 were calibrated and found out that the temperature difference was less than half a degree (OESTREICH, 2017). This way, it was chosen not to calibrate the others, as these errors would not affect the final system performance of the data analysis. The calibration of these 6 PT-100 can be found at the annex B.

#### 4.1.2.2 Solar Radiation Transducer

A Kipp & Zonen pyranometer, model CMP21, was installed on the same angle of the solar collectors. This pyranometer was calibrated by the manufacturer and is used to obtain tilted solar radiation data in order to validate the simulations in the future. Figure 13 is a picture of the pyranometer installed on the test bed. The solar radiation transducer is wired directly to the Agilent data-logger.



Figura 13 – Pyranometer installed on the test bed.

#### 4.1.2.3 Flow Meter

A Omega FPR303 flow meter was installed on the inlet tube of the testbed. Since there is only one inlet to the test bed used by both system, it is possible to track down the outlet flux by monitoring the flow meter. Thus, the FPR303 is used to control the amount of water that is released every hour following the water consumption profile. This Flow meter is factory calibrated, its accuracy is 1% of full scale. Its K-factor is 436 pulse per gallon, which can be converted to 8.68 milliliters per pulse. Differently from the others measurement equipments, the flow meter is wired directly to the Arduino chip-set, which also controls the solenoid valves, applying the same hot water consumption profile used on the simulations.

### 4.1.3 System Control Apparatus

The test bed is a long run experiment and, to operate it properly, the whole system is controlled by a computer. The solenoid valves, the computer and the Agilent data-logger are not required on the final product since there will be less measurement and automation equipments installed on the system. Thus, only Arduino, or a similar chip-set may be needed to log the household's hot water consumption, the solar radiation measurements and to control the heating devices.

#### 4.1.3.1 Solenoid Valves

Three Solenoid valves were installed on the experiment rig. Two valves control the outlet of each system, and one valve control the inlet of the testbed. An example of solenoid valve installed on the test bed is represented on figure 14



Figura 14 – SDWHS solenoid Valve.

#### 4.1.3.2 Arduino

Arduino is, according to the distributor (ARDUINO, Acessado em 20/07/2017), "an open-source electronics platform based on easy-to-use hardware and software". However, as stated on their website: "physically embedding an Arduino board inside a commercial product does not require you to disclose or open-source any information about its

design". Thus, it is safe to use an Arduino board and not disclose some information about programming on a future product.

The Arduino Uno board was selected due to its low price and its capabilities are in line with what is required for this test bed. The ports needed were: one five Volts port, on ground port and four digital ports. Three digital ports were used to wire the Solenoid valves. For the flow meter the ground, the five volts and one digital port were used. Figure 15 shows the wired Arduino.

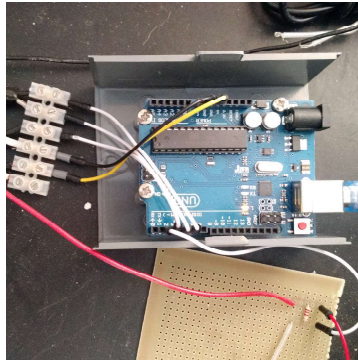


Figura 15 – The Wired Arduino uno board of the test bed.

#### 4.1.3.3 Agilent 34972A Data-logger

An Agilent data-logger model 34972A is used to log the temperature and radiation transducers. This data-logger has a higher accuracy when compared to an Arduino uno board. It has 0.004% basic Vdc accuracy, low reading noise and scan rates up to 250 channels/sec. These data-loggers are used to monitor multiple signals (temperature, voltage, etc.) over extended periods of time to identify irregularities. On figure 16 is a photo of the data-logger used on the test bed.

#### 4.1.4 System Control Procedure

The automated control of the system was implemented on LabVIEW environment. LabVIEW is a system-design platform and development environment, it is commonly used for data acquisition, instru-

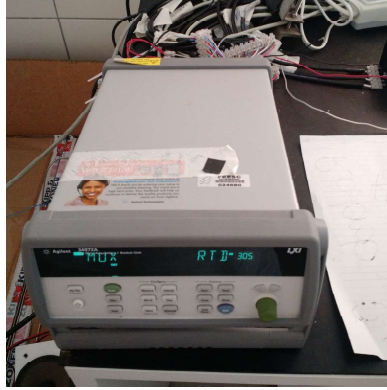


Figura 16 – The Wired Agilent 34972A data-logger of the test bed.

ment control, and industrial automation. It has a visual programming language that allows for a intuitive and easy programming and automation of devices. Two different strategies are implemented on the code. One uses the last day's data as a prediction for the next day's conditions; the other uses delivers a constant amount of heat every day. On the appendix C there is an image of the whole program created on LabVIEW environment, and some pieces of the program are going to be explained there.

## 4.2 EXPERIMENTAL DATA

The simulation validation will be presented here comparing results from the test bed and obtained by the simulation for selected days. Figure 17 shows the position of each temperature transducer on the PSDWHS side of the test bed.

### 4.2.1 Simulation Validation

Even though there were several problems with the test bed functionality throughout the tested time, it was possible to use the available data to validate the TRNSYS simulation. This validation was the main goal of building the test bed. Once the TRNSYS simulation is validated with experimental data it is possible to use this simulation to calculate

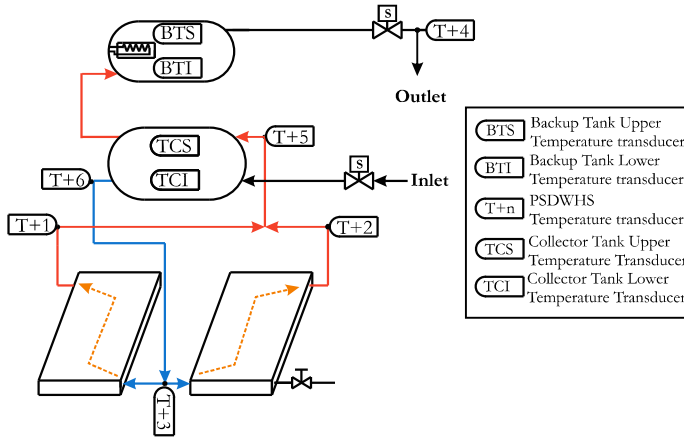


Figura 17 – Temperature transducers name and position.

how the system will behave at other cities, using other control strategies or using different simulated weather forecast.

There are two main TRNSYS Types that must be validated: The Type 533, which corresponds to the backup tank; and the Type 45a which corresponds to the collector tank and the solar collectors altogether.

#### 4.2.1.1 Backup Tank validation: Type 533

In order to validate the Type 533 for this work simulation the test bed backup tank was subjected to a heat loss experiment. The simulation must be able to emulate the tank behaviour under the same conditions. Figure 18 shows the temperature decrease for 2 points inside the backup tank.

By analyzing figure 18 it is possible to estimate the backup tank stratification profile. The top temperature is estimated at  $70^{\circ}\text{C}$  as it is the maximum temperature of the T+4 temperature transducer. The T+4 temperature transducer is the PT-100 installed at the outlet of the Backup tank as shown on figure 17. From there, a simple linear function is used until the upper backup tank temperature transducer initial data of  $64.03^{\circ}\text{C}$ . From the upper to the lower temperature transducer a different linear function is used since the temperature gradient

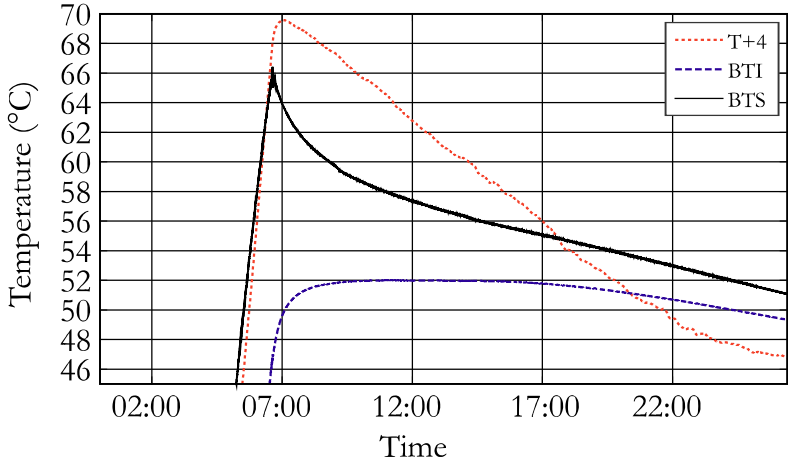


Figure 18 – Temperature on the backup tank for the heat loss experiment on June 05

is much more aggressive. Finally from the lower temperature transducer until the bottom of the tank another linear function is used for the stratification function. This function has the same slope as the function of the first section of the tank.

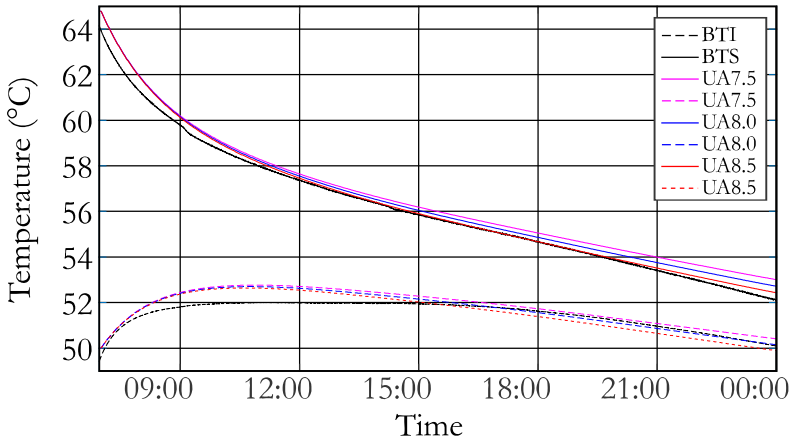


Figure 19 – Backup tank validation - Values for June 05



The simulation was carried out using as input the above mentioned stratification profile and three different global loss coefficient (UA). Figure 19 show these results alongside the experimental data for comparison. Global loss coefficient of  $8 \text{ kJ}/\text{hm}^2\text{K}$  was selected as the results obtained using this value were closer to the experimental data.

For comparison purposes the global tank loss coefficient was obtained in two other ways. One using equation 4.1, and the other by numerically deriving the Tank temperature - equation 4.2. These approaches, however, did not deliver adequate values. The values obtained were:  $3.6\text{kJ}/\text{hm}^2\text{K}$  and  $5.3\text{kJ}/\text{hm}^2\text{K}$  from the theoretical equation and the experimental temperature derivation respectively.

$$UA = \frac{2\pi k_i D_s}{S_s \log\left(\frac{D_s + 2e_i}{D_s}\right)} + \frac{2\pi k_i D_s^2}{4e_i} \quad (4.1)$$

$$UA = \frac{\frac{dE}{dt}}{T_m - T_\infty} \quad (4.2)$$

Figure 20 shows an out of sample validation that was carried out for Type 533. This figure shows that Type 533 was able to emulate the real system behaviour described by the test bed data for June 15 using the selected input parameters.

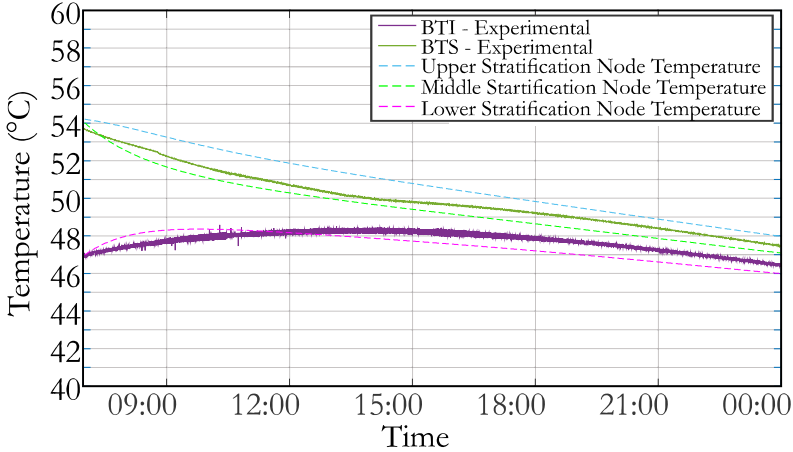


Figura 20 – Backup tank out of sample validation - Values for June 15

#### 4.2.1.2 Collector Tank Validation: Type 45a part 1

The same approach as before was used on validation of the tank simulation of Type 45a. The collector tank was subjected to a heat loss experiment.

Figure 21 shows the temperature decrease for 2 points inside the collector tank. The black line is the Average between the lower section of the experimental tank temperature (TCI) and the upper section of the experimental tank temperature (TCS). The figure shows the collector tank temperature decrease for June 13 at 18:00 to June 14 at 06:00. However, between 18:00 and 21:00 there is a thermal inertia effect. The heat loss temperature profile for this situation should follow an exponential or a linear rule, but, there is a thermal capacitance influence that the model could not simulate.

Again, an out of sample validation was carried out for June 12 to June 13. On June 13, a non identified event happens at 01:00. However, the temperature decrease lines from experimental and simulated data have similar angular coefficient, therefore, this event should not effect this validation.

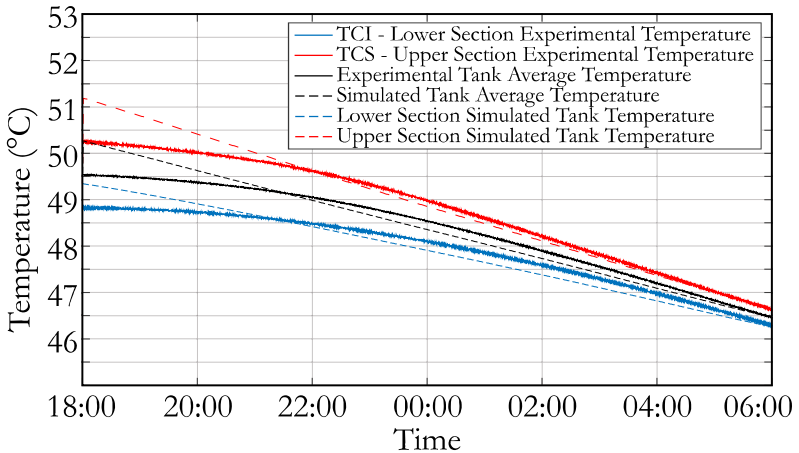


Figura 21 – Temperature on the Collector tank for the heat loss experiment on June 13 and 14

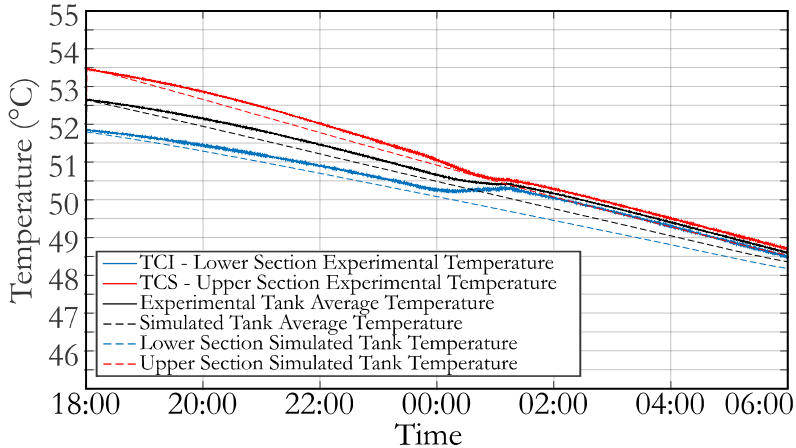


Figura 22 – Collector Tank out of sample validation - Values for June 12 and 13

#### 4.2.1.3 Collector Validation: Type 45a part 2

Before going through the collector analysis, the boundary conditions have to be outlined. Therefore the global solar radiation on tilted surface calculated by TRNSYS and measured on the test bed were compared. TRNSYS uses a sky model as well as global radiation on horizontal surface to obtain the  $G_t$  values. The global radiation on horizontal surface data were obtained by the BSRN (Baseline Surface Radiation Network) meteorological station that is also located at the Rooftop of LEPTEN.

Figure 23 shows both the  $G_t$  obtained by the test bed and  $G_t$  calculated by the TRNSYS program. This image shows that TRNSYS program followed perfectly the experimental trend. Since the boundary conditions match, one could focus on validating the collector simulation. Figure 24 shows the collector's outlet temperature variations for June 15.

As seen on figure 24 one collector has a much higher temperature than the other, however the mix temperature is following the lower temperature collector trend. This indicates that one collector had mass flow blockage. In order to address to this blockage, an energy balance was carried out at mixing point.

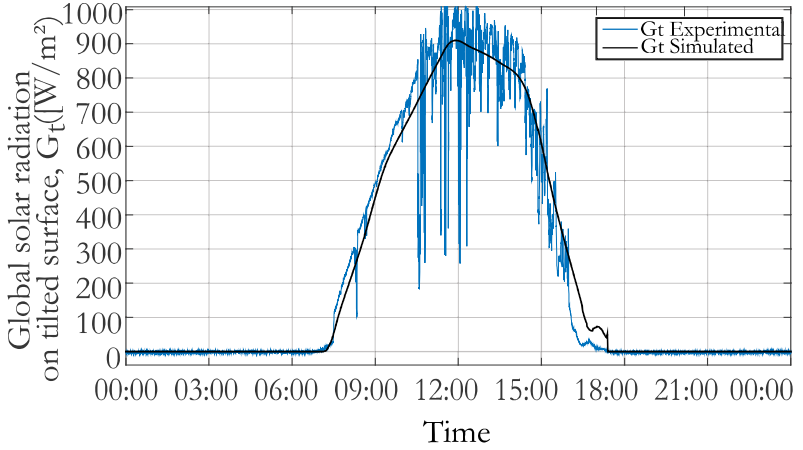


Figure 23 –  $G_t$  from experiment and  $G_t$  from TRNSYS for June 15

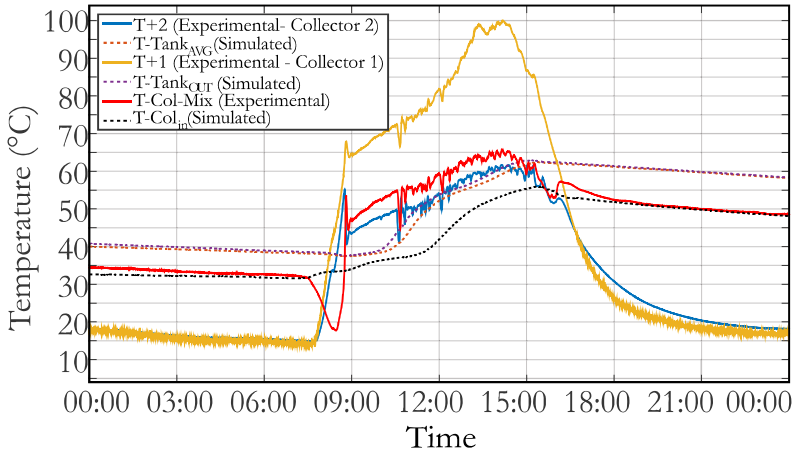


Figure 24 – Simulated and Experimental Collector temperature for June 15

$$T_{mix}\dot{m}_{mix} = T_1\dot{m}_1 + T_2\dot{m}_2 \quad (4.3)$$

Even though there is no information about the mass flow rate

from the collector, it is possible to make a scale analysis in order to find an effective collector area to be used on the simulation. The effective area is directly proportional to the mass flow rate proportion between the two collectors and, thus, it represents a correction factor for the collector's absorption properties.

$$\dot{m}_{mix} = \dot{m}_1 + \dot{m}_2 \rightarrow \frac{\dot{m}_2}{\dot{m}_{mix}} = 1 - \frac{\dot{m}_1}{\dot{m}_{mix}} + \quad (4.4)$$

and then

$$T_{mix} = T_1 \frac{\dot{m}_1}{\dot{m}_{mix}} + T_2 \left( 1 - \frac{\dot{m}_1}{\dot{m}_{mix}} \right) \quad (4.5)$$

isolating  $\frac{\dot{m}_1}{\dot{m}_{mix}}$

$$\frac{\dot{m}_1}{\dot{m}_{mix}} = \frac{T_m - T_2}{T_1 - T_2} \quad (4.6)$$

Then, one can define effective area as:

$$EA = 1 + \frac{\dot{m}_1}{\dot{m}_{mix}} \rightarrow EA = 1 + \frac{T_m - T_2}{T_m + T_1} \quad (4.7)$$

Figure 25 shows the values for the effective area calculated for June 15. The average value is 1.4 and was used on the simulation in order to account for this mass flow block on one of the collectors.

Back to figure 24, the dashed lines are the tank and collector temperatures for the simulation. The simulation results were able to emulate the collector curve trend. The initial drop on mixture temperature is due to cold water on the tubes, effect of heat loss at night.

In order to ensure that the collector parameters and program are following the experimental trend an out of sample validation was again carried out. Figures 27 and 26 presents the effective area and collector temperatures respectively.

#### 4.2.1.4 Simulated System Validation

The simulation was carried out for two different days, one in summer conditions, and other in winter conditions. For each of these days the effective collector area was calculated and found to be equal to  $1.5m^2$ .

Comparison on the incident solar radiation on tilted surface was

also carried out, and TRNSYS values followed the experimental trend. Figures 28 and 29 shows the solar incident radiation on tilted surface for the selected days.

In order to validate these simulations the parameters obtained on previous sections were used. Also, for this simulation the hot water load profile was forced to be equal to experimental values. Since the input parameters and boundary conditions are close to experimental values, the simulation was expected to deliver results close to experimental values. First figures for collector temperatures are shown, then the collector tank temperatures, and at last the backup temperatures are presented.

As stated by Salazar (2004) (SALAZAR, 2004) and confirmed by figures 30 and 31, the computational code used by TRNSYS does not take into account capacitance effects. Therefore, at the start and the end of the day, simulated values have a greater variations than experimental ones. The greater oscillation found on the end of the day on figure 31 are due to numeric error on TRNSYS. This error however, does not affect much the other simulated values since the thermosiphon flow rate is zero after sunset.

Figures 32 and 33 presents simulated and experimental values for collector tank temperature. The experimental values are obtained on the middle of the tank, just above and below its center. Simulated

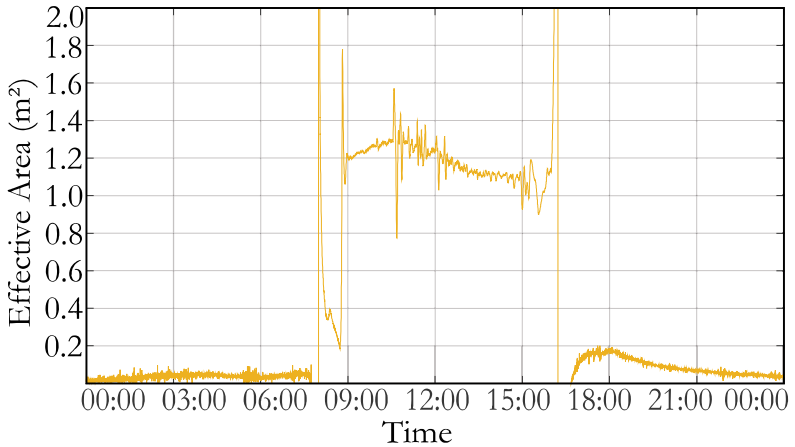


Figura 25 – Effective Area for June 15

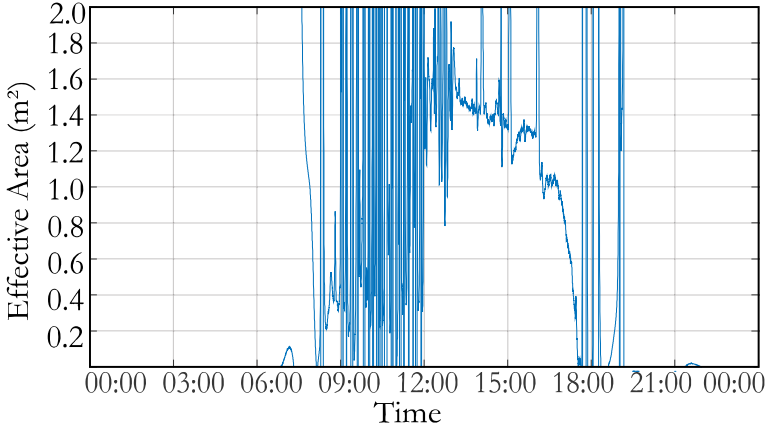


Figure 26 – Effective Area for January 19

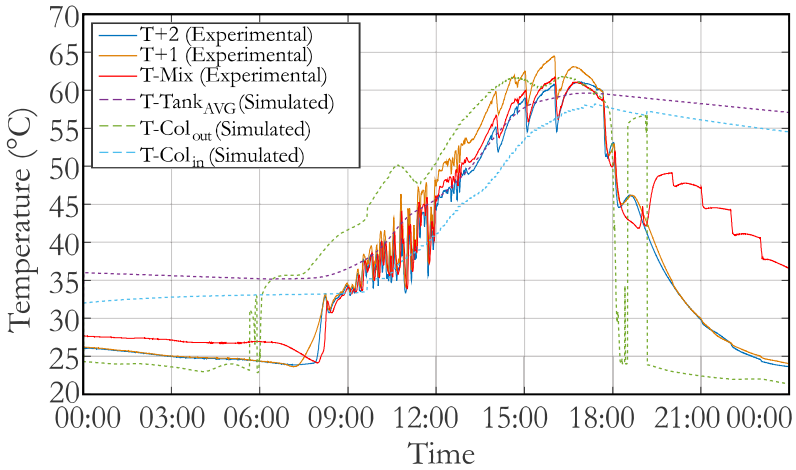


Figure 27 – Simulated and Experimental Collector temperature for January 19

values, on the other hand, are obtained on outlet to backup tank and outlet to collector. Therefore the simulated collector tank temperature at outlet are higher than the upper experimental collector tank temperature. But, as it is compared to the experimental backup upper tank

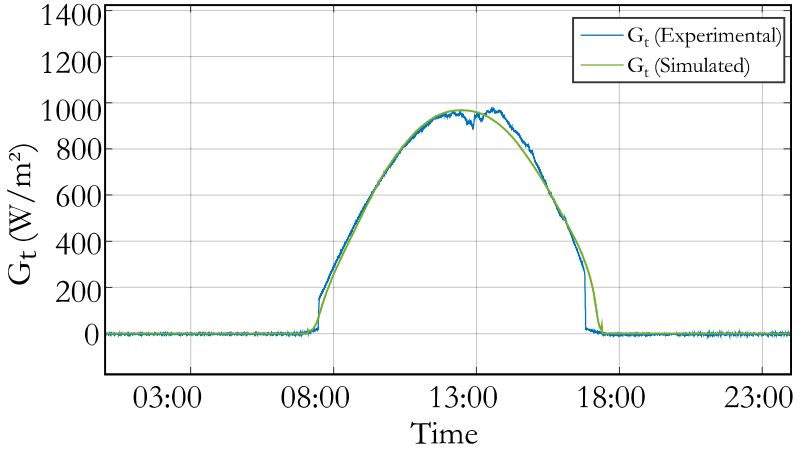


Figura 28 –  $G_t$  comparison for June 11

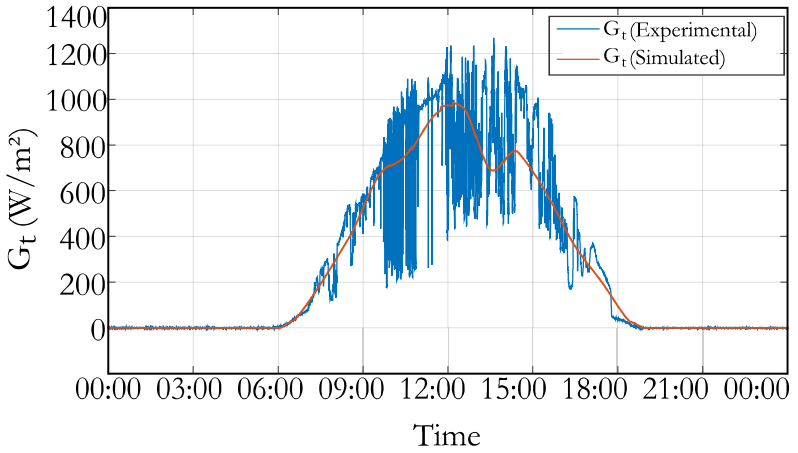


Figura 29 –  $G_t$  comparison for February 22

temperature its values are similar, as expected. The same happens for february 22<sup>nd</sup>.

The temperature difference between experimental and simulated values is also verified on figures 34 and 35. On these figures again the position of the temperature transducer is the answer. On the test



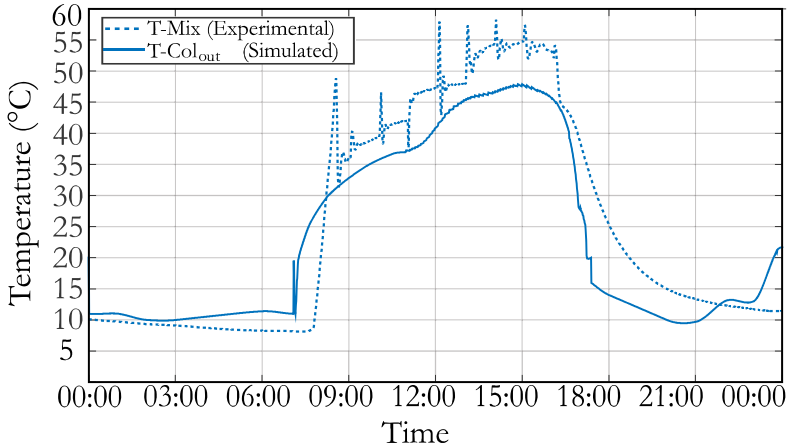


Figure 30 – Collector Temperature for June 11

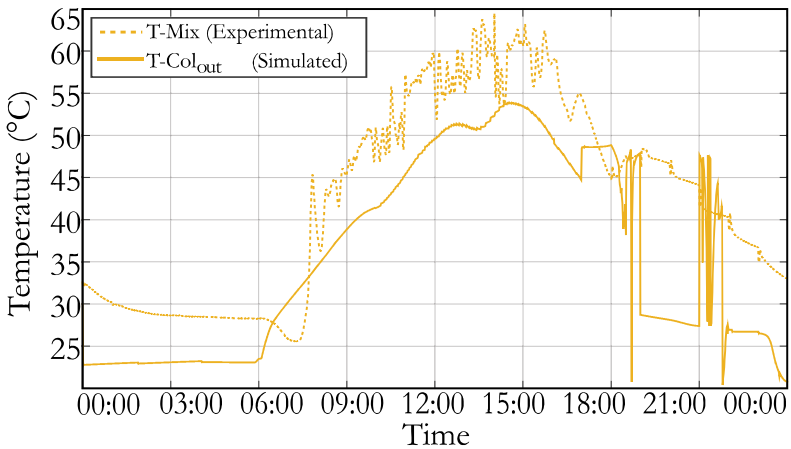


Figure 31 – Collector Temperature for February 22

bed the temperature transducers are just above and below the auxiliary heater, which is installed on the middle of the tank. The temperature data on simulation however, is obtained on the outlet and as an average tank temperature.

Although the simulated temperature trend seems out of place,

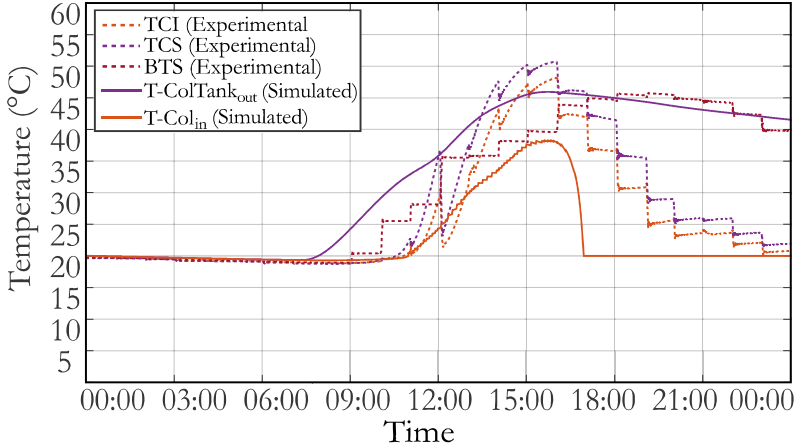


Figure 32 – Collector Tank Temperature for June 11

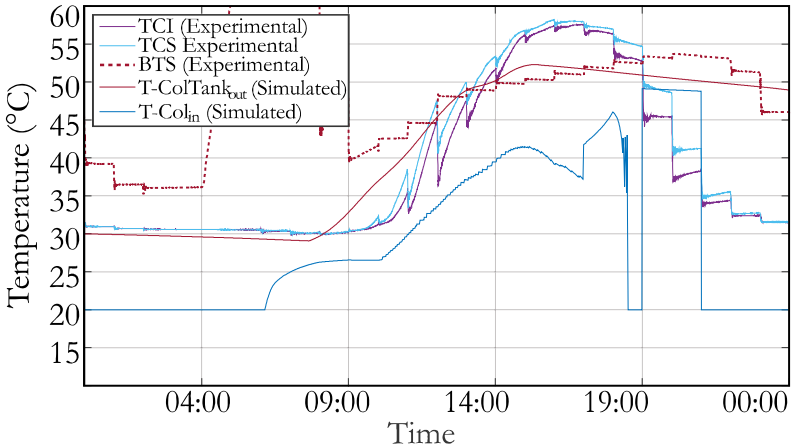


Figure 33 – Collector Tank Temperature for February 22

the solar fraction, total absorbed energy and auxiliary energy are close to experimental values. There is an expected difference, however, on the solar gain and on the solar fraction once it was not possible to access it directly on the test bed. To do so, a flow meter on the collector outlet would be needed.

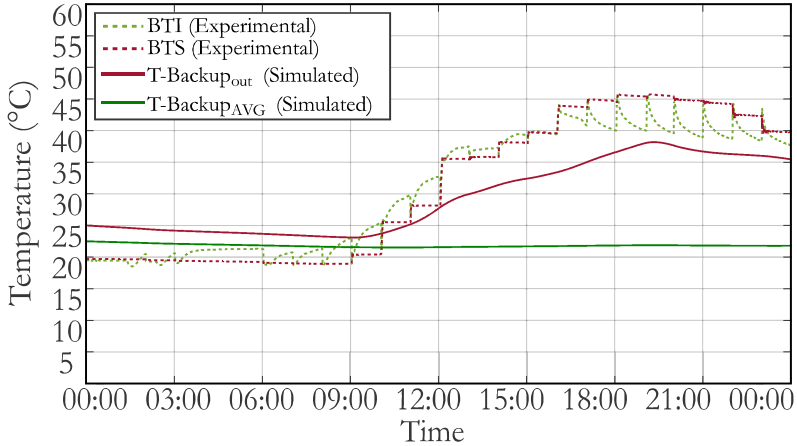


Figura 34 – Backup Tank Temperature for June 11

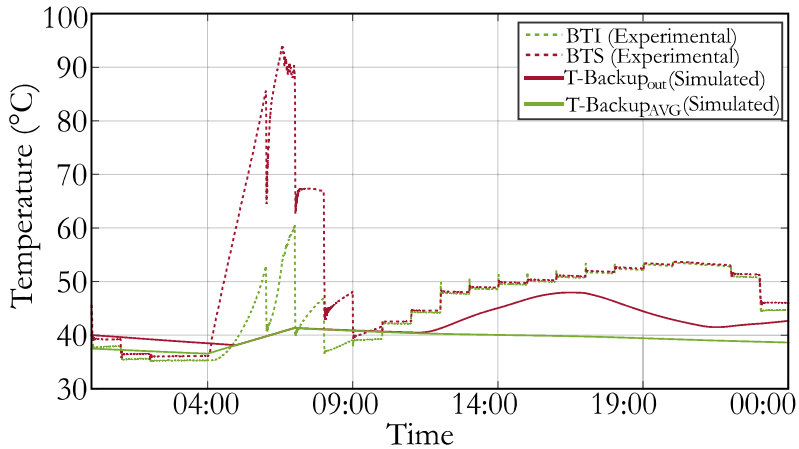


Figura 35 – Backup Tank Temperature for February 22

The solar Fraction is given by equation 2.2,  $S_F = \frac{Q_s}{Q_L}$ . It is a ratio between the solar energy gain and the auxiliary energy needed when solar collector area is zero (Duffie and Beckman - 2006) (DUFFIE; BECKMAN, 2006).

The testbed does not have a flux meter on the tubes that lead

to the solar collector, thus, the author is not able to perform an energy balance on the solar collector. In order to calculate the solar fraction, one must change the solar fraction equation using an energy balance on the system.

The objective is to calculate such value using the available data from the testbed. To obtain the solar fraction, first the amount of heat absorbed by the collector has to be accessed indirectly. From equation 2.2 it is possible to describe:

$$Q_S + Q_{aux} = Q_{Load} + Q_{losses} \quad (4.8)$$

where  $Q_{losses}$  are all the possible heat losses from the testbed,  $Q_{Load}$  is the energy used to deliver hot water to the consumer,  $Q_{aux}$  is the total auxiliary heating energy and  $Q_S$  is the solar energy gain. This equation can be written as:

$$Q_S = Q_{Load} + Q_{losses} - Q_{aux} \quad (4.9)$$

Applying equation 4.9 on solar fraction equation, 2.2:

$$S_F = \frac{Q_{Load} + Q_{losses} - Q_{aux}}{Q_{Load}} \quad (4.10)$$

The auxiliary energy input of the test bed can be easily obtained by analyzing the amount of time the electric heaters were on, and checking if the consumed water was above 39°C. The system load, however, is dependent of the heat losses over the day and the user's hot water demand. Thus, the author chose to modify the solar fraction to ease the calculations. As a result, the modified solar fraction ( $M_{SF}$ ) takes into account the amount of energy used on a shower head for the user load profile, neglecting, energy losses. The system's tank and tubes, however, are insulated from the outside, hence, those heat loss are pondered to be minimal. This is, also, a conservative approach since the obtained estimate representing the solar fraction is less than the real value. Then, the modified solar fraction is given by:

$$M_{SF} = 1 - \frac{Q_{aux}}{Q_{showerL}} \quad (4.11)$$

where,  $Q_{showerL}$  is given by:

$$Q_{ShowerL} = M \cdot c \cdot \Delta T. \quad (4.12)$$

as "M" is the total hot water mass load for the system, namely 200

liters, "c" is the water specific heat, and " $\Delta T$ " is 19°C corresponding for a temperature difference from 20°C to 39°C.

In this fashion it was possible to calculate the modified solar fraction of the systems for validation days. Values for total daily tilted incident radiation ( $G_t$ ), total auxiliary energy ( $Q_{aux}$ ), total required load energy ( $Q_{Shower}$ ), and the solar fraction ( $M_{SF}$ ) for June 11<sup>th</sup> and February 22<sup>nd</sup> days are found on tables 2 and 1 respectively.

Tabela 1 – Values for 22 of February

|              | $G_t$    | $Q_{Shower}$ | $Q_{Aux}$ | $M_{SF}$ |
|--------------|----------|--------------|-----------|----------|
| Experimental | 23756.50 | 15884        | 10428     | 34%      |
| Simulated    | 23485.91 | 15884        | 10800     | 32%      |

As seen on table 1 values for total required load energy are very high. This is due to the fact that the test bed was using fixed pre-heating strategy. Values for solar fraction for June 11<sup>th</sup> (table 2), otherwise are much better, however, on this day pre-heating was not required. Since these are values for a day these do not represent a monthly behaviour. As stated before, the test bed must still undergo a long term experiment in order to obtain such data.

Tabela 2 – Values for 11 of June

|              | $G_t$ | $Q_{Shower}$ | $Q_{Aux}$ | $M_{SF}$ |
|--------------|-------|--------------|-----------|----------|
| Experimental | 23615 | 15884        | 2649      | 83%      |
| Simulated    | 23865 | 15884        | 10800     | 89%      |

## 5 SIMULATION RESULTS

The PSDWHS was simulated for five different Brazilian cities. First, results for Florianopolis will be shown and compared to results from other authors for the same city. Then results for the other 4 cities will be shown and compared with each other and with results for Florianopolis.

### 5.1 FLORIANOPOLIS

For the case where there is no weather forecast errors, Carminatti (2014) obtained a solar fraction of 87%, way above the value achieved by Koller (2012), Gonçalves (2014) and Passos (2011) whose results were 68%, 74% and 73% respectively. This case takes into account that the weather forecast is flawless and the system is able to predict perfectly all the meteorological variables of the day, in other words, this is the ideal case.

Carminatti defends its solar fraction values arguing that Passos used an analytical formulation for the system. This means that Passos had to use a full mixed tank model, which lowers the thermal gain in the collector by rising its inlet temperature. While taking on Koller's results, Carminatti states that Koller assumes that, for every day, the lowest backup tank temperature would happen at 4 am, which is not always true. Hence in Koller's simulation there are days that an electric shower is needed to keep the temperature above 39°C even in the ideal case. Carminatti, comparing its results with Gonçalves, states that the Gonçalves heat losses are higher, and since Gonçalves storage tanks are 50 liters smaller its average tank temperature is higher and, as consequence, its solar collector efficiency decreases.

#### 5.1.1 Florianopolis previous day strategy and weather forecast strategy

For comparison purposes the author used Koller's control strategy and obtained a solar fraction of 85%, a higher value than Koller's, above-mentioned, 68%. Figure 36 shows that this strategy could shift the electric energy demand peak, transferring to dawn the auxiliary energy needed when there is not enough solar energy. Figure 37 shows

Carminatti (2014) results for the PSDWHS working with a weather forecast control system with errors ranging from 10% to 50%. This means that errors in weather forecast lead to progressively higher over-estimation of the energy received by the solar collector. It is worth remembering that this simulation used noise generator to emulate the weather prediction and its errors, thus it is not a real weather forecast.

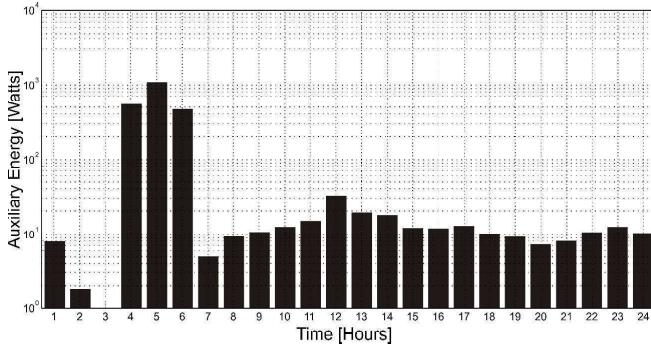


Figure 36 – Auxiliary Energy consumption for every hour of the day.

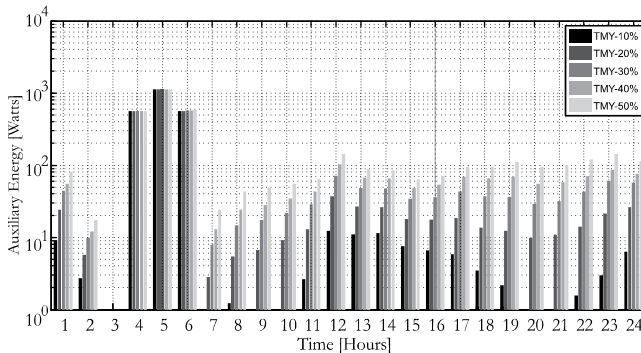


Figure 37 – Year Average Auxiliary Energy Consumption for every hour using asymmetrical square random distribution for the simulation of weather forecast for Florianopolis. TMY-50% means that forecasted radiation was 100% higher than real values.

Comparing figure 36 and 37 illustrates that Koller's control strategy is good and can be compared to Carminatti's results for the case

where solar radiation is 20% less than expected in weather forecast.

## 5.2 RESULTS FOR OTHER CITIES

First Results for Koller's control strategy will be shown for each city, compared to each other and discussed. Then Carminatti's approach will be used, results will be shown and compared to each other and to Koller's approach.

### 5.2.1 Koller's Control Strategy

Figure 38 shows results for equal days' strategy for each city. Differently from what was described earlier, Florianopolis was not the most disfavored city for the PSDWHS using this control strategy.

Figure 38 also shows that for peak hours Curitiba and Santa Maria also uses more auxiliary energy than Florianopolis. Both cities are in Brazilian uplands and have a colder weather than Florianopolis which is an island on the coast of Santa Catarina. Thus, this result is expected since both cities, Curitiba and Santa Maria, have a colder weather when compared to Florianopolis.

To better analyze the graph from figure 38 one should look at the climate normal for Florianopolis and Sao Paulo. Climate normal is a long period average for weather variables, it is usually used thirty years of data to create these averages. The newest Brazilian climate normal is from 1961 to 1990 (BRASIL., 1992). The graph from figure 39 shows the climate normal for the *number of three or more consecutive dry day's period* for each month. For instance, if there were more consecutive dry days on a month for a city in comparison to another city, then, one can conclude that one city would have less weather variability than the other, for the analyzed data points.

In this case the graph from figure 39 compares two cities: Florianopolis and two places in Sao Paulo. For at least seven months Florianopolis had more consecutive dry days, on this thirty year average, than Sao Paulo. This means that, on average, one can assume that Florianopolis climate is less variable than Sao Paulo's. This can explain why the equal days strategy delivered worse results for Sao Paulo than for Florianopolis. One must remember that, for Koller's control strategy, it is not only important to have good solar radiation, but also to have little weather variability, since it uses the past day as



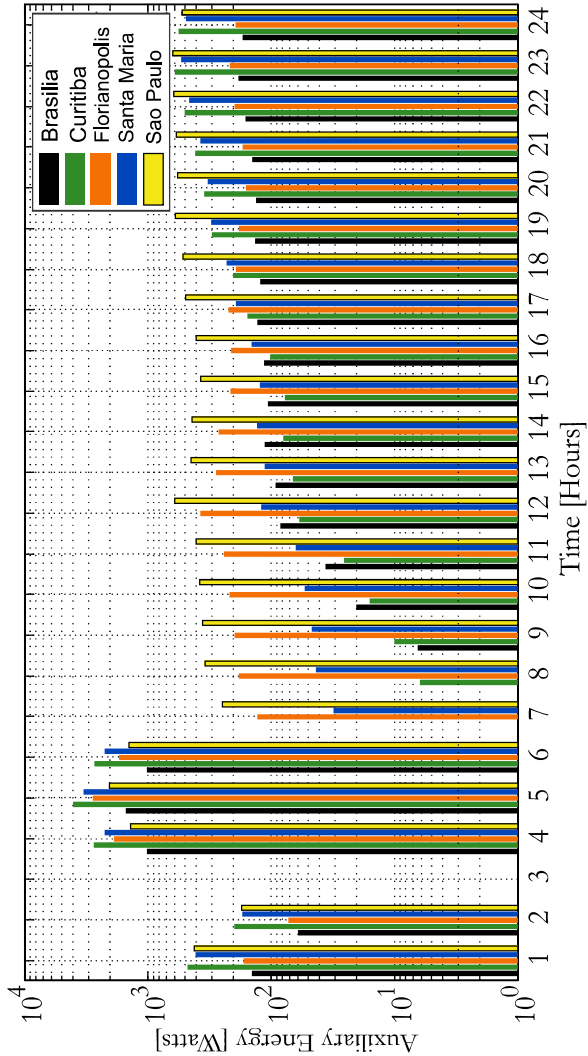


Figura 38 – Year Average Auxiliary energy consumption for every hour using equal days strategy. Comparison between Florianopolis, Sao Paulo, Brasilia, Santa Maria and Curitiba.

an input to calculate the pre-heating energy for the next day.

In figure 40 is a graph of the climate normal for sunshine hours

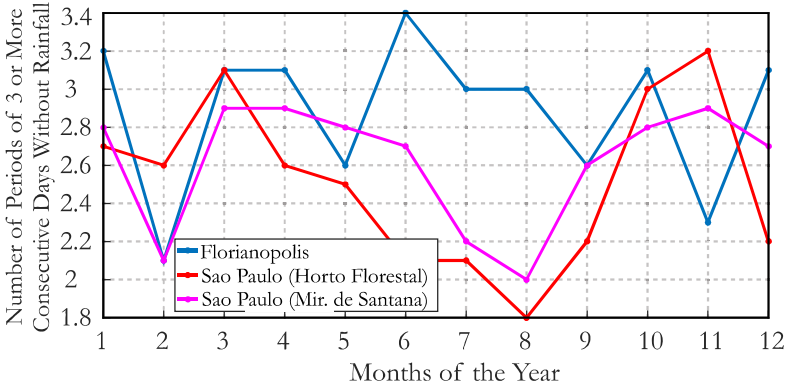


Figure 39 – A comparison of two different cities for number of 3 or more consecutive dry day’s period.

for Florianopolis and Sao Paulo. Although this does not indicate numerically the amount of irradiation in these cities, it does give a glimpse on the irradiation behavior. Thus, one can conclude from the graph that Florianopolis has less irradiation than Sao Paulo. In other words, Florianopolis may have less solar radiation but its weather has less variability when compared to Sao Paulo and this explains the unpredicted behavior of the equal day’s control strategy observed on figure 38.

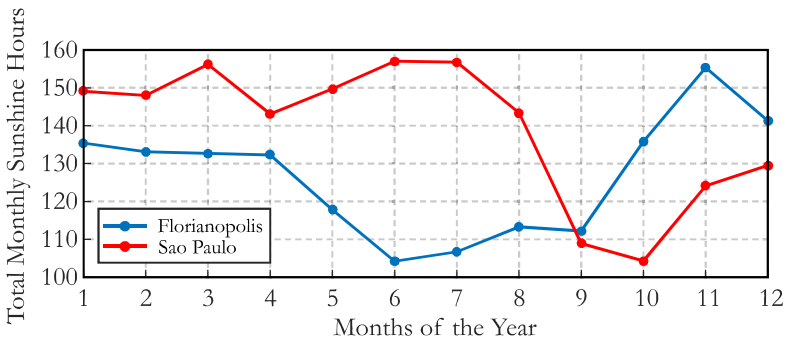


Figure 40 – Comparison between Florianopolis and Sao Paulo sunshine hours.

## 5.2.2 Weather Forecast Strategy

A different approach is going to be presented in this section. It consists on using Kollers Year Fraction/Energy Fraction graphic to demonstrate how the system is affected by the simulated weather forecast errors. In his work, Koller used this graph to analyse the effect of hot water consumption overload on the system.

Thomas Koller explains the energy fraction as follows:

"The energy fraction gives information on how much electric energy is needed during the peak hours for the days that require electric energy, due to an overrated solar radiation. The energy fraction is defined as the electric energy that is needed during the peak hours divided by the electric energy that would be necessary if the whole amount of water was heated by an electric shower"

Therefore, it is natural that this approach should be used to analyse the results from the simulated weather forecast strategy.

On Figures 41, 42, 43, 44, 45, there are the year fraction/energy fraction graphics for all studied cities, for 10%, 20%, 30%, 40%, 50% simulated weather forecast errors respectively.

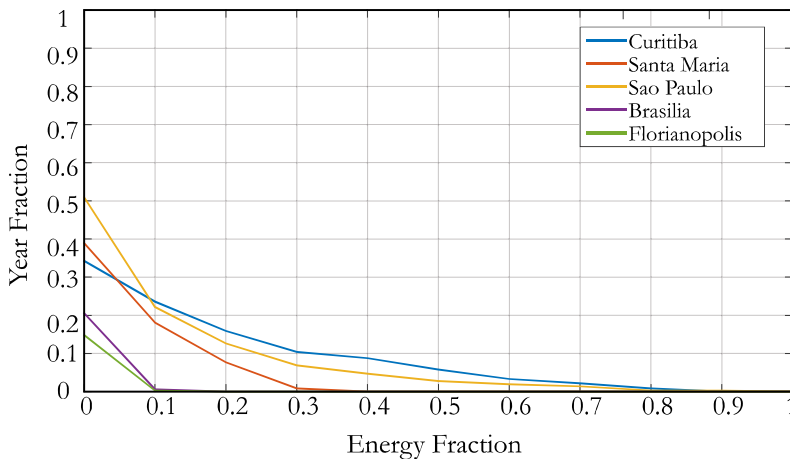


Figura 41 – Energy Fraction Year Fraction graph for 10% simulated weather forecast errors.

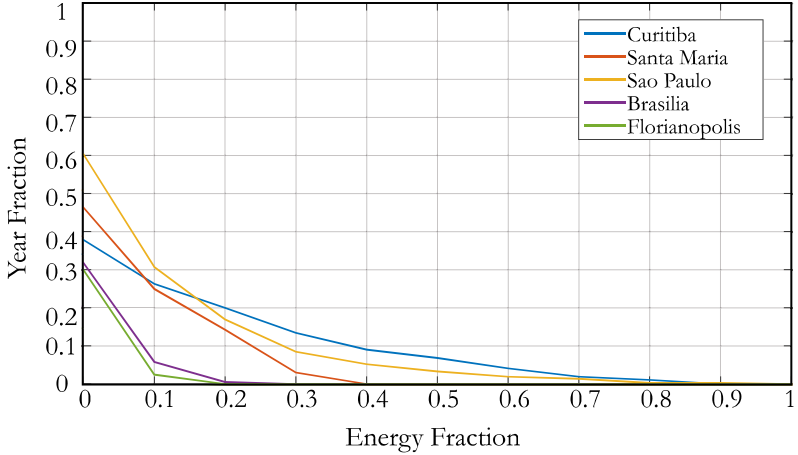


Figura 42 – Energy Fraction Year Fraction graph for 20% simulated weather forecast errors.

The observation of the results shows that even for 10% simulated forecast error, for Sao Paulo, half the days of the year need auxiliary energy at peak hours. However, only 22% of the days, for the same parameters, need more than 10% of the energy that would be necessary without the PSDWHS.

Also, the graphics presented in these figures shows that for all cities, besides Curitiba, all curves quickly flatens even when the simulated forecast errors reach 50%. For these cities, when the simulated forecast errors reach 50%, only Sao Paulo has more than 10% of the days of the year that uses more than 10% of Energy Fraction. Therefore, one can conclude that the system could shift the demand peak for all cities, besides Curitiba. In other words, this shows that this systems can reduce the energy demand peak if greatly used in these cities households.

On figures 46, 47, 48, 49, 50 are the same graphics presented before, but now the curves for the same city are shown together. Here one can see the effect of the increasing simulated forecast errors on the PSDWHS behavior for each city.

Some slightly abridged graphics are shown on figures 51, 52, 53, 54 and 55. These graphics synthesises the 10 graphs presented before, as they show, on the "X" axis, the increase of simulated weather forecast errors, on the "Y" axis, the year fraction, and the curves on the graphics are for the designated energy fraction for each city. Put differently,

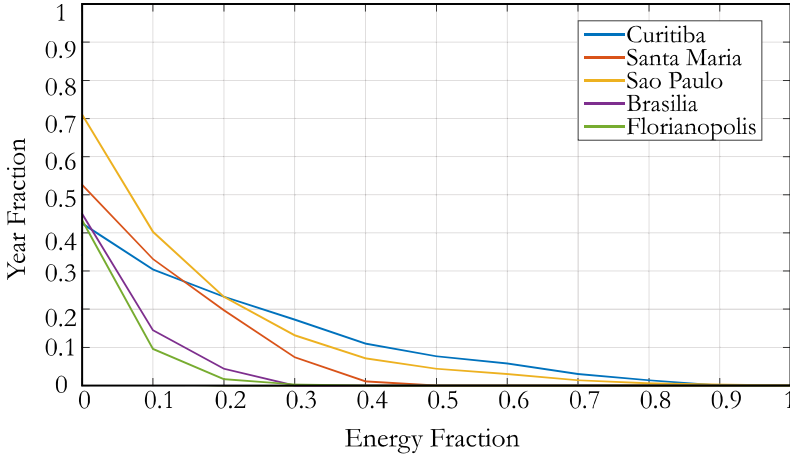


Figura 43 – Energy Fraction Year Fraction graph for 30% simulated weather forecast errors.

these figures shows that as the simulated forecast errors increases, the system fails to deliver hot water to the user more often. However, these curves were built in order to search for a tendency that could justify a stopping point on increasing the accuracy of the weather forecast, and not to demonstrate a rather obvious outcome. Figures 52 and 53 are ideal for the purpose.

By analysing figure 52 for example, one can conclude that for Florianopolis and Brasilia a 20% simulated weather forecast error causes less than 10% of year fraction to have 20% or more energy fraction. This means that for these cities a PSDWHS using a Weather forecast that misses by 20%, would have less than 10% of the days of the year that would need 20% or more of the energy that would be necessary without the PSDWHS at peak hours. Thus, this graphic method is useful in order to choose how accurate a real weather forecast has to be for this system to be functional.

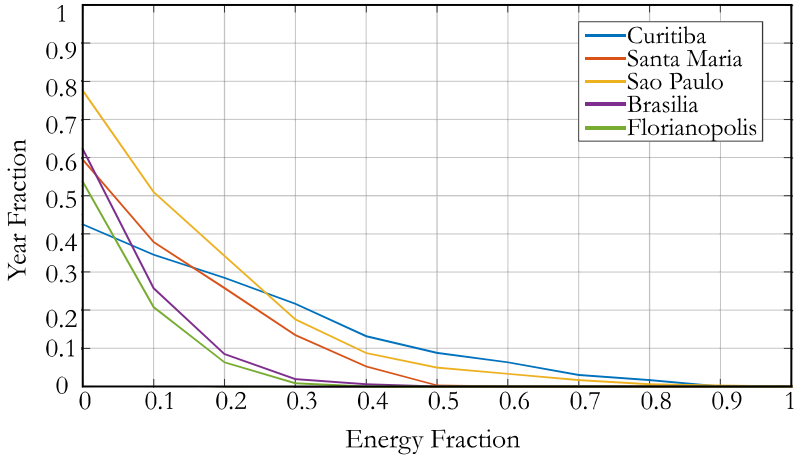


Figura 44 – Energy Fraction Year Fraction graph for 40% simulated weather forecast errors.

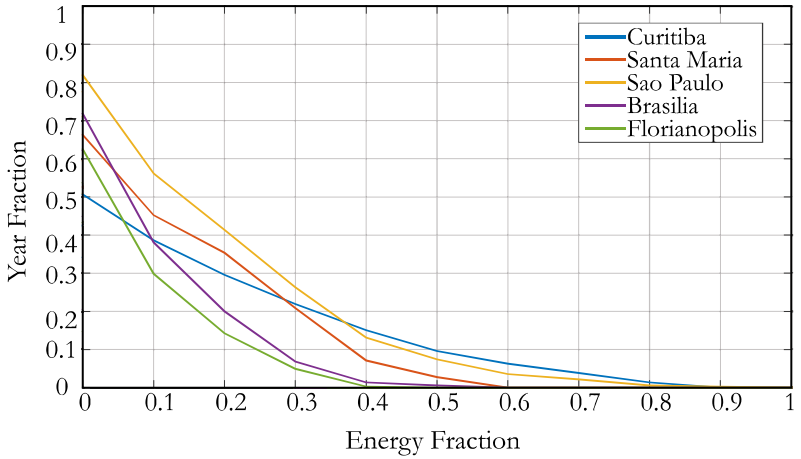


Figura 45 – Energy Fraction Year Fraction graph for 50% simulated weather forecast errors.

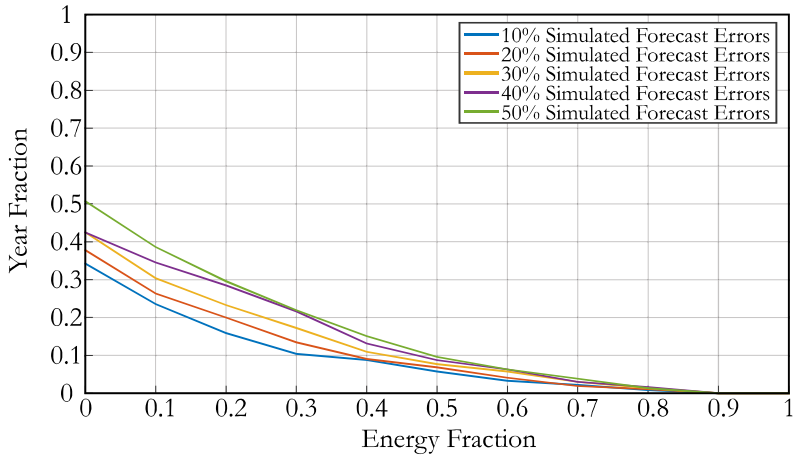


Figure 46 – Energy Fraction Year Fraction graph for Curitiba.

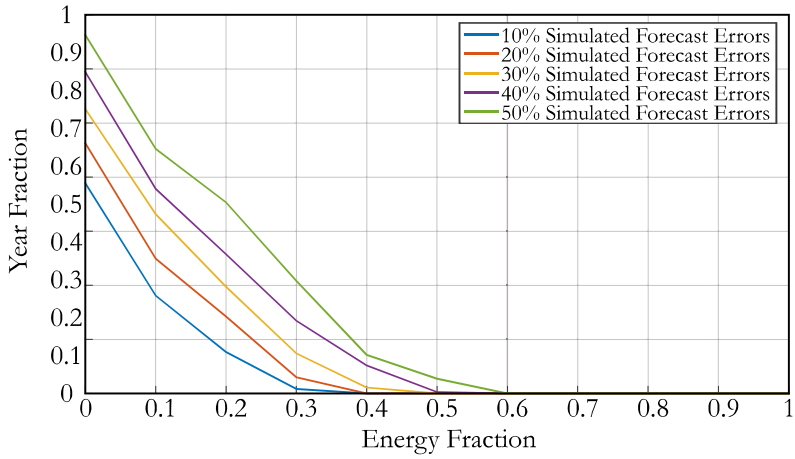


Figure 47 – Energy Fraction Year Fraction graph for Santa Maria.

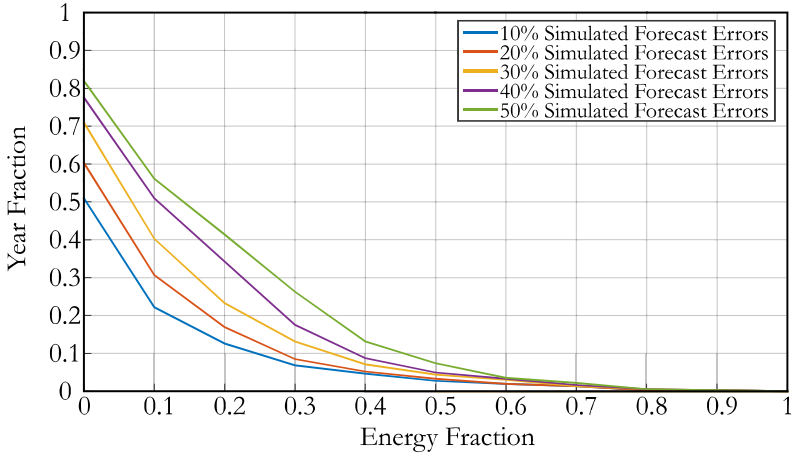


Figura 48 – Energy Fraction Year Fraction graph for Sao Paulo.

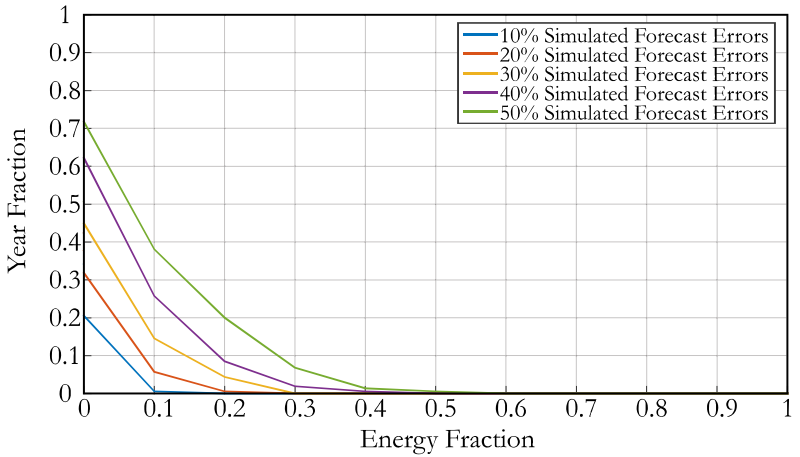


Figura 49 – Energy Fraction Year Fraction graph for Brasilia.



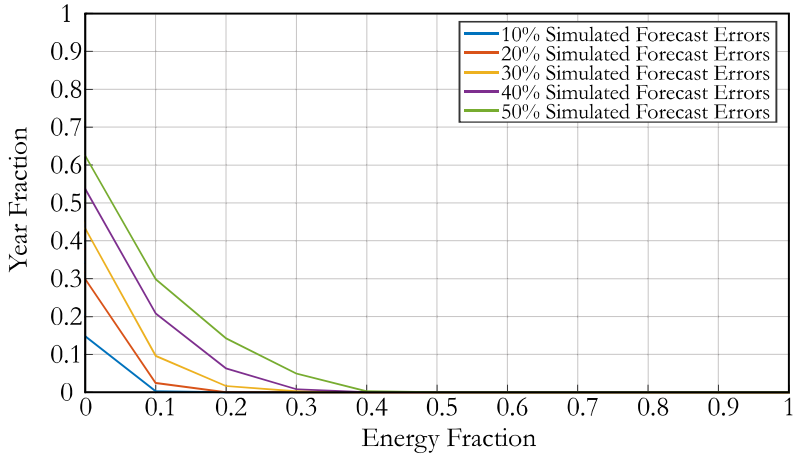


Figura 50 – Energy Fraction Year Fraction graph for Florianopolis.

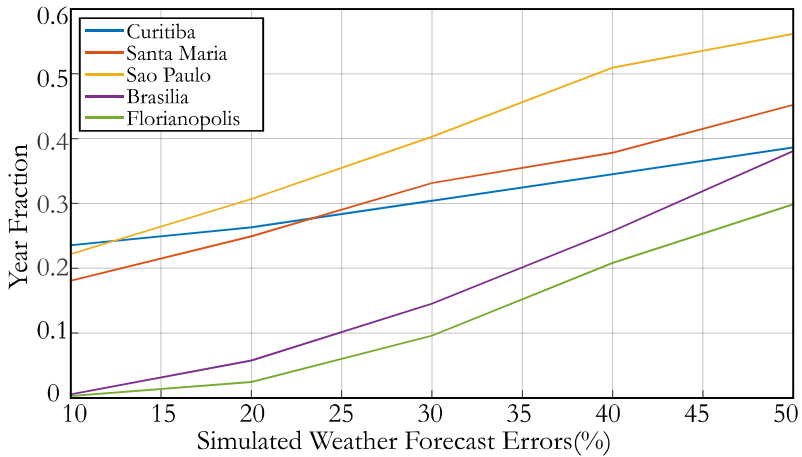


Figura 51 – Simulated forecast Errors Effect on Year fraction for 10% Energy Fraction.

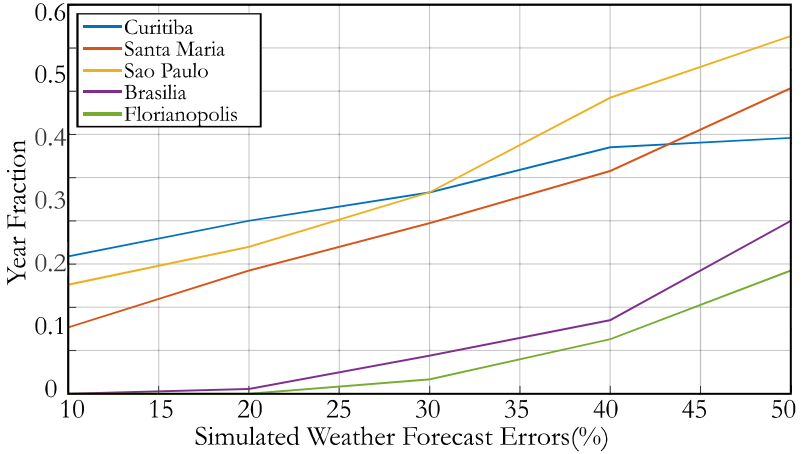


Figura 52 – Simulated forecast Errors Effect on Year fraction for 20% Energy Fraction.

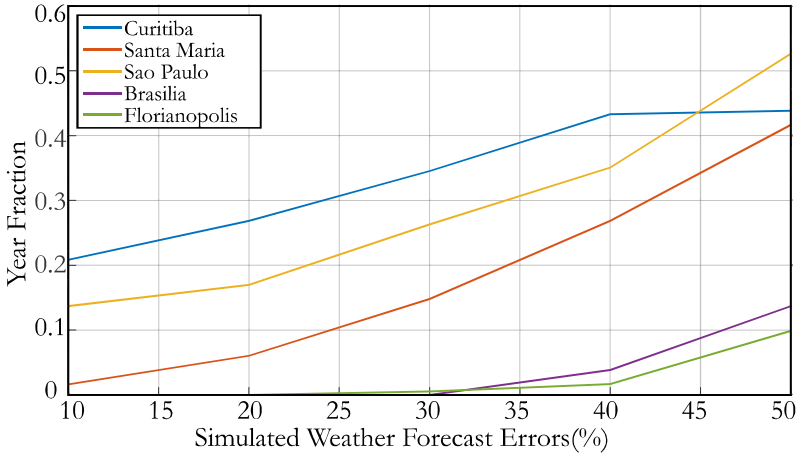


Figura 53 – Simulated forecast Errors Effect on Year fraction for 30% Energy Fraction.

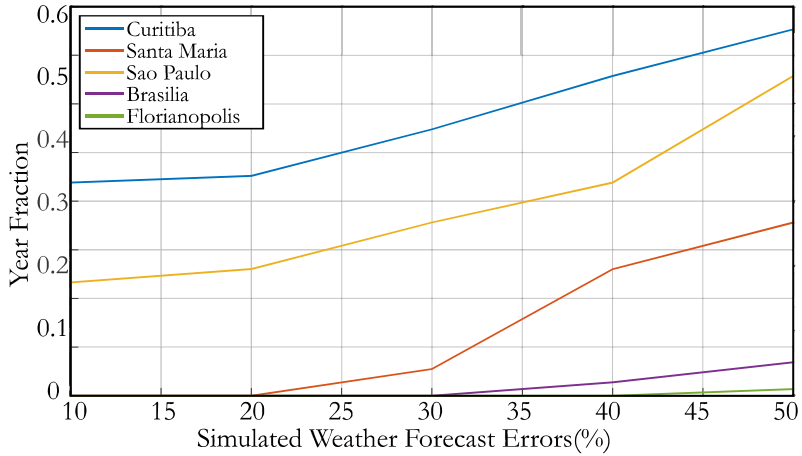


Figure 54 – Simulated forecast Errors Effect on Year fraction for 40% Energy Fraction.

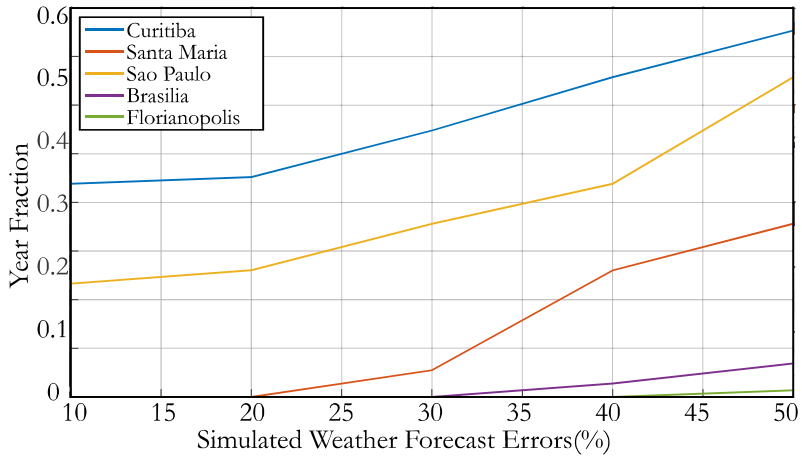


Figure 55 – Simulated forecast Errors Effect on Year fraction for 50% Energy Fraction.

## 6 CONCLUSIONS FUTURE WORKS AND SUGGESTIONS

From the second law of thermodynamics point of view the electric shower is an inefficient device. It destroys the potential to generate work, in other words it destroys exergy. This device accounts for 43% of the electric energy demand peak. Therefore, a country that plans to use its energy sources consciously has to use electric heating as a backup system only. The present work presented a system design that was able to shift and shrink the energy demand peak for hot water of a household by implementing a weather forecast controlled solar domestic water heating system.

The objectives presented on this work were achieved since it was possible to obtain data from the test bed and to validate the TRNSYS simulation. Also the carried out simulations delivered expected data and proved that the system may be used in many Brazilian regions shifting the energy demand peak of a dwelling.

It is concluded through the simulations that the control system could work even with unreliable meteorological information, managing to shift and attenuate the electric energy demand peak of a residence. This guarantees a great contribution to the electric energy distribution company, once and if such a system were to be largely employed in Brazil, it would be possible to shift or shrink the electric energy demand peak of the whole network. For the energy company this would mean a significant reduction of costs, since it would no longer be necessary to oversize the power grid or overload the plants.

Another outcome was the graphics from figures 51, 52, 53, 54 and 55. These figures showed that as the simulated forecast errors increased, the system failed to deliver hot water to the user more often. This was an expected behavior. However, these graphs were built in order to search for a tendency that could justify a stopping point on increasing the accuracy of the weather forecast. However, more research must be done in order to trace down such stopping point.

Since the simulation is validated, a suggestion for future works is to change the profile of the random distribution used to simulate the weather forecast errors to a more realistic one. Another approach would be using different real weather forecast with different known errors and again use this dissertation method to choose which weather forecast method is better suited for the system's pre-heating control strategy.

Despite it was not possible to obtain long term data from the test bed, a full scale rig of the system was built and its simulation could be validated. In order to obtain long term data, the test bed must go through some modifications. First, its tanks must be changed or modified since the installed devices have a high global loss coefficient ( $8kw/hm^2K$  and  $5kw/hm^2K$  for the backup and collector tank respectively). Second, the tubes from the collector must be checked in order to search for a water flow block as seen trough transducers temperature differences on figure 24. This blockage may be created by soldering material or plumber's tape on tube walls. And at last, change the control board, or its program, in order to increase reliability.

Although the Arduino uno chip-set is being used, a personal computer and an Agilent data-logger are still needed to control the test bed. In order to create a cheaper product the data-logger and the PC should be removed from the system and their functionality should be absorbed by the arduino uno, duo or mega, or simmilar chip-set - rasperry pi is also a good choice. These small chip-sets can be upgraded to have a integrated wireless board to connect to the internet through the house Wi-Fi. Doing so will allow the system to obtain the weather forecast from a server. Thingspeak open data server is also a good choice for data logging and data analysis since it is fully integrated to MATLAB and arduino board.

The presented results indicate that the system could work even with unreliable meteorological information. More research must be carried out in order to access the correct method for weather forecast to be used on the pre-heating strategy. The test bed has to, still, get through a long term experiment in order to obtain experimental data on solar fraction, and electric energy demand peak shift.

## REFERÊNCIAS

- ARDUINO. Disponível em: <<http://www.arduino.cc>>, Acessado em 20/07/2017.
- BOLAND, J. Time-series analysis of climatic variables. *Solar Energy*, v. 55, n. 5, p. 377–388, 1995.
- BOLAND, J. The importance of the stochastic component of climatic variables in simulating thermal behavior of domestic dwellings. *Solar Energy*, v. 60, n. 6, p. 359–366, 1997.
- BOLAND, J.; DIK, M. The level of complexity needed for weather data in models of solar system performance. *Solar Energy*, v. 71, n. 3, p. 187–198, 2001.
- BRASIL. Normais climatológicas (1961-1990). *Ministerio da Agricultura e Reforma Agraria (MARA), Brasilia, Brasil*, 1992.
- CARMINATTI, H. S. Análise dos efeitos dos erros da previsão meteorológica em um sistema de aquecimento solar de Água doméstico com duplo tanque e com sistema de controle de pre-aquecimento. *TCC (Graduacao) - Curso de Engenharia Mecânica, Centro Tecnológico, Universidade Federal de Santa Catarina, Florianópolis*, 2014.
- COLLE, S. et al. Uma análise de sistemas de aquecimento solar de água para uso doméstico no Brasil. *III Congresso Brasileiro de Energia Solar*, 2010.
- DUFFIE, J. A.; BECKMAN, W. A. Solar engineering of thermal processes, third edition. John Wiley & Sons, p. 908, 2006.
- FESTA, R.; RATTO, C. F. Proposal of a numerical procedure to select reference years. *Solar Energy*, v. 50, n. 1, p. 9–17, 1993.
- GONCALVES, J. E. Análise de um sistema solar assistido por bomba de calor direcionado a aquecimento doméstico de água. *TCC (Graduacao) - Curso de Engenharia Mecânica, Centro Tecnológico, Universidade Federal de Santa Catarina, Florianópolis*, 2014.
- GRÜNENFELDER, W. J.; TÖDTLI, J. The use of weather predictions and dynamic programming in the control of domestic hot water systems. *MELECON, Mediterranean electrotechnical conference*, 1985.

HOLLANDS, K. G. T.; D'ANDREA, L. J.; MORRISON, I. D. Effect of random fluctuations in ambient air temperature on solar system performance. *Solar Energy*, v. 42, n. 4, p. 335–338, 1989.

INMAN, R. H. et al. A smart image-based cloud detection system for intrahour solar irradiance forecasts. *Journal of Atmospheric and Oceanic Technology*, v. 31, n. 10, p. 1995–2007, 2014.

JANNUZZI, G. D. M.; SCHIPPER, L. The structure of electricity demand in the brazilian household sector. *Energy Policy*, v. 19, n. 9, p. 879–891, 1991.

KLEIN, S. et al. Trnsys 17: A transient system simulation program. *Solar Energy Laboratory, University of Wisconsin, Madison, USA*, 2010.

KOLLER, T. Simulation and performance analysis of a solar domestic hot water system controlled by weather forecast information. *TCC (graduacao) - Curso de Engenharia Mecanica, Centro Tecnológico, Technische Universität München, Florianopolis*, 2012.

OESTREICH, J. Estudo da condensação em convecção natural de superfícies híbridas (superhidrofóbicas e hidrofílicas). *Dissertação (Mestrado) - Curso de Pós Graduação em Engenharia Mecanica, Centro Tecnológico, Universidade Federal de Santa Catarina, Florianopolis*, 2017.

ONS. Operador nacional do sistema elétrico. *Disponível em:* <http://http://www.ons.org.br/>, Date Accessed: 20/07/2017.

PASSOS, L. Um estudo sobre impactos técnicos e econômicos da agregação do aquecimento solar de água nos domicílios brasileiros. *Dissertação (Mestrado) - Curso de Engenharia Mecanica, Centro Tecnológico, Universidade Federal de Santa Catarina, Florianopolis*, 2011.

PRUD'HOMME, T.; GILLET, D. Advanced control strategy of a solar domestic hot water system with a segmented auxiliary heater. *Energy and Buildings*, v. 33, p. 463–475, 2001.

SALAZAR, J. P. Economia de energia e redução do pico da curva de demanda para consumidores de baixa renda por agregação de energia solar térmica. *Dissertação (mestrado) - Universidade Federal de Santa Catarina*, 2004.

SANCHO, J. M. et al. Solar radiation atlas for spain based on surface irradiance data from eumetsat climate monitoring-saf. AEMET - Spanish Meteorological Agency, p. 8, 2012.

SKEIKER, K. Comparison of methodologies for tmy generation using 10 years data for damascus, syria. *Energy Conversion and Management*, v. 48, n. 7, p. 2090–2102, 2007.

SWERA. Solar and wind energy resource assessment. *Disponível em: <<http://swera.unep.net/>>*, 2001.

VIVAUDOU, S. Investigation of the possible implementation of weather forecast and demand prediction in a smart control scheme for solar domestic hot water systems. *Dissertation (Master) - Sustainable Engineering: Renewable Energy Systems and the Environment, University of Strathclyde, Glasgow*, 2014.

WIRTH, H. Recent facts about photovoltaics in germany. Fraunhofer Institute for Solar Energy Systems ISE, p. 88, 2017.





## **APÊNDICE A – Test Bed Hydraulic Design**



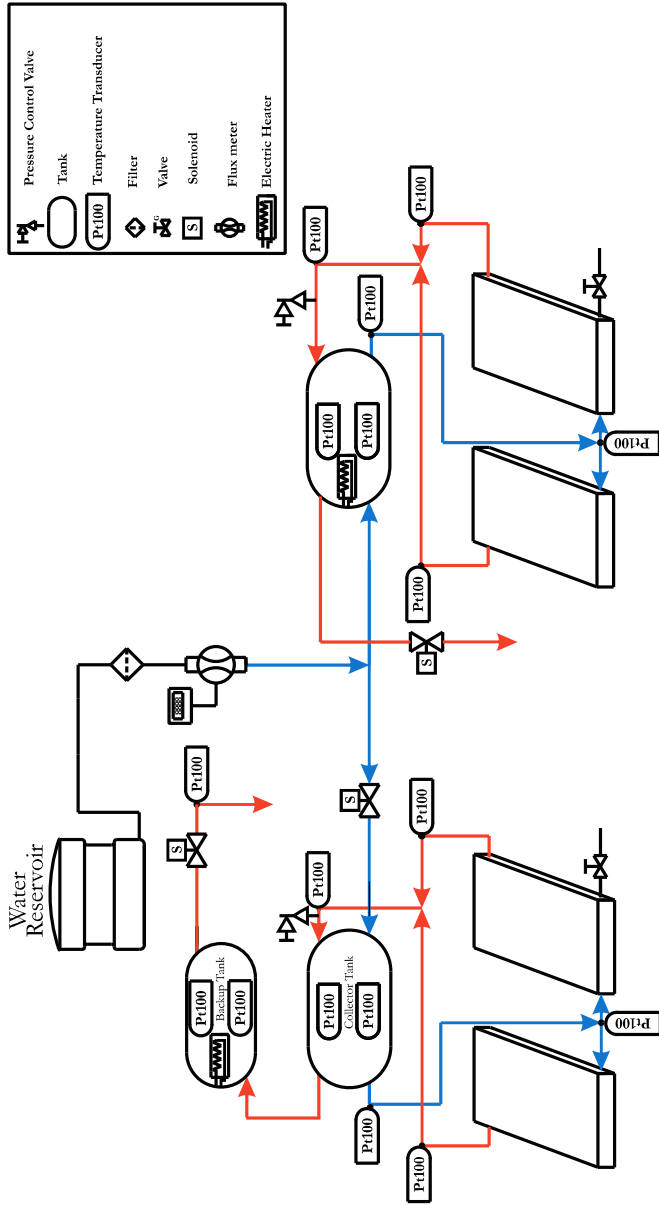


Figura 56 – Test bed Hydraulic Design.



## APÊNDICE B - Test Bed Electric Design



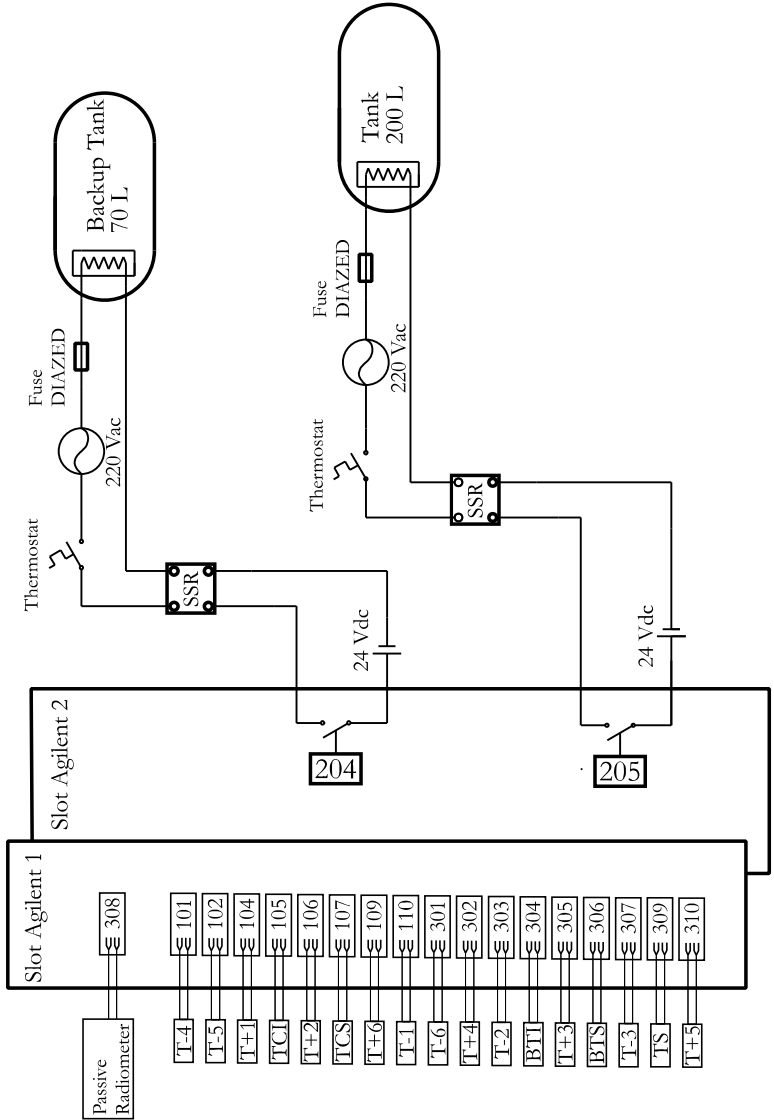


Figura 57 – Test bed Electric Design.



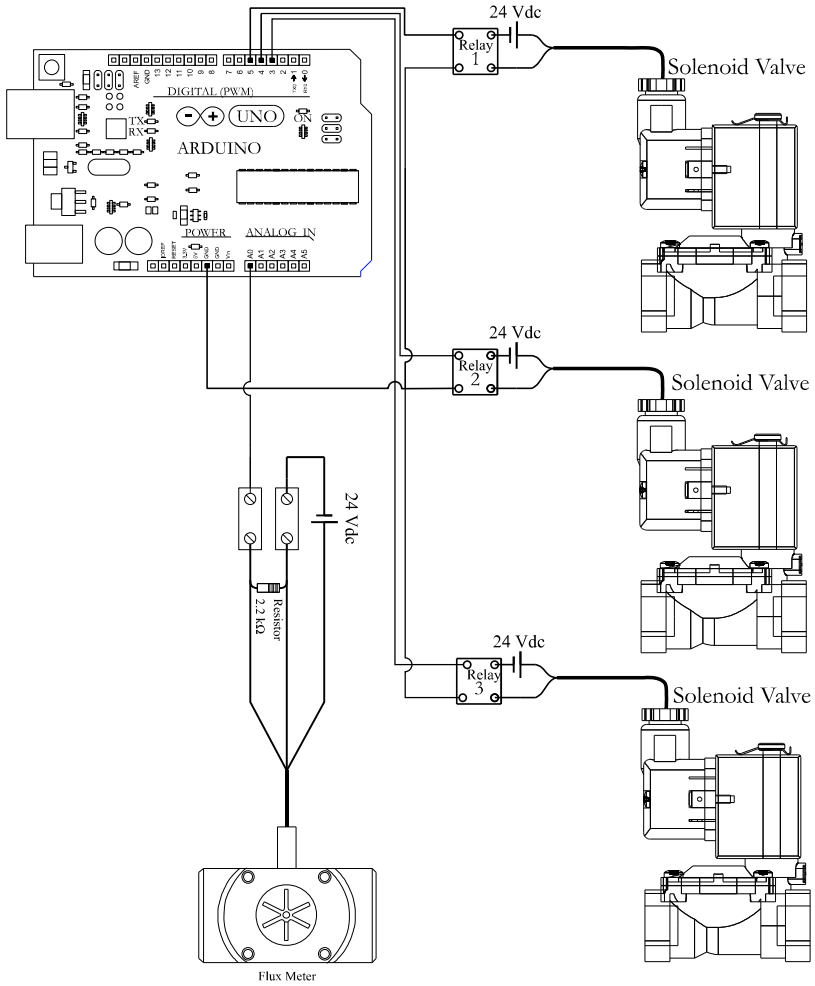


Figura 58 – Test bed Electric Design.

## **APÊNDICE C - Labview: System Control Procedure**



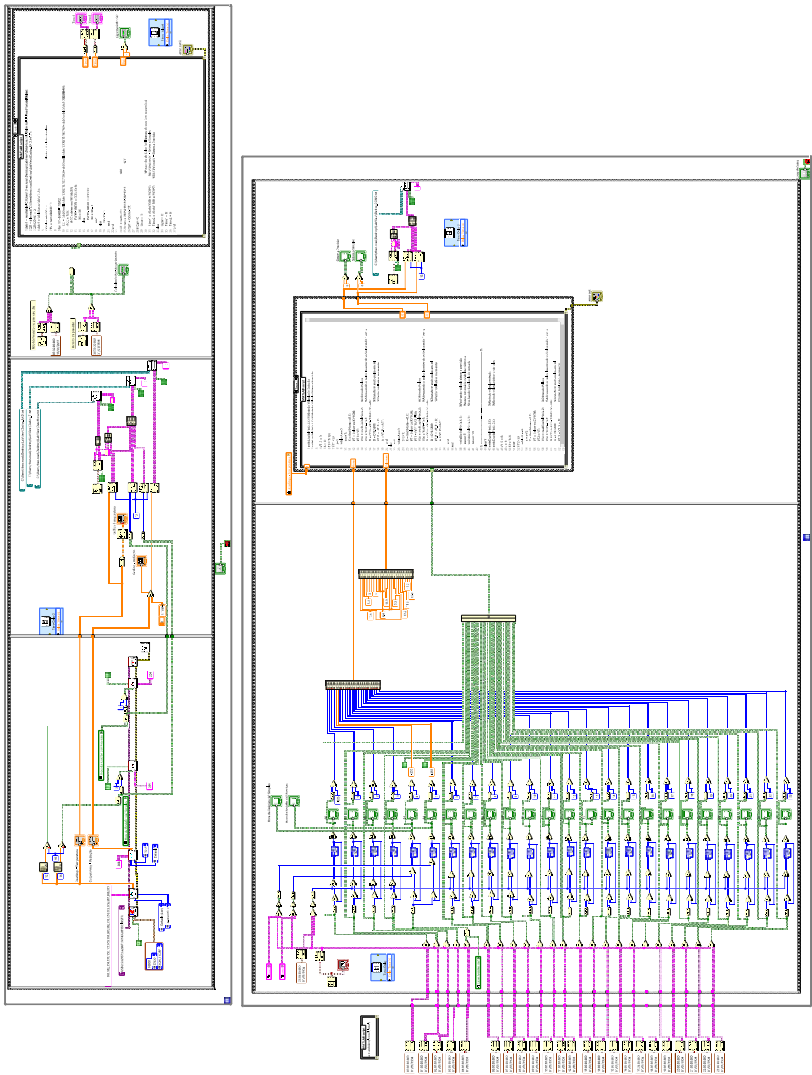


Figura 59 – Test bed control LABVIEW program.

### C.1 QUICK EXPLANATION OF THE PROGRAM

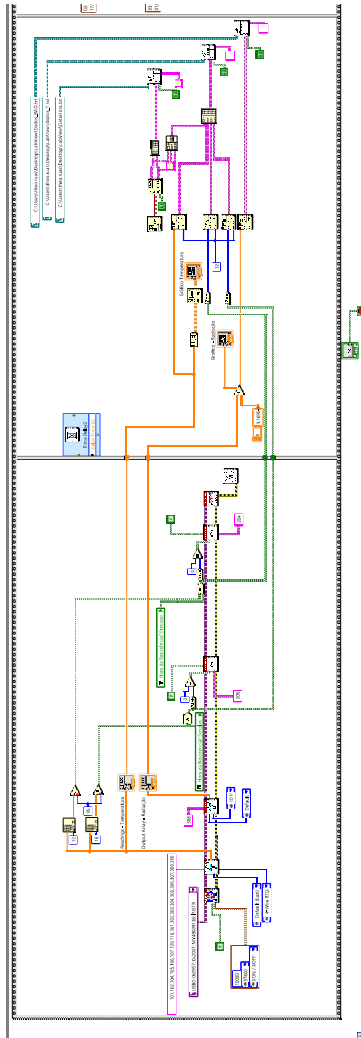


Figura 60 – Temperature and radiation data-logging.

On figure 60 is the first piece of the program. It is where the temperature and radiation data-logging is programmed for the Agilent

34972A. In this part the auxiliary heaters are controlled and safety a limit for the tank temperature is set.

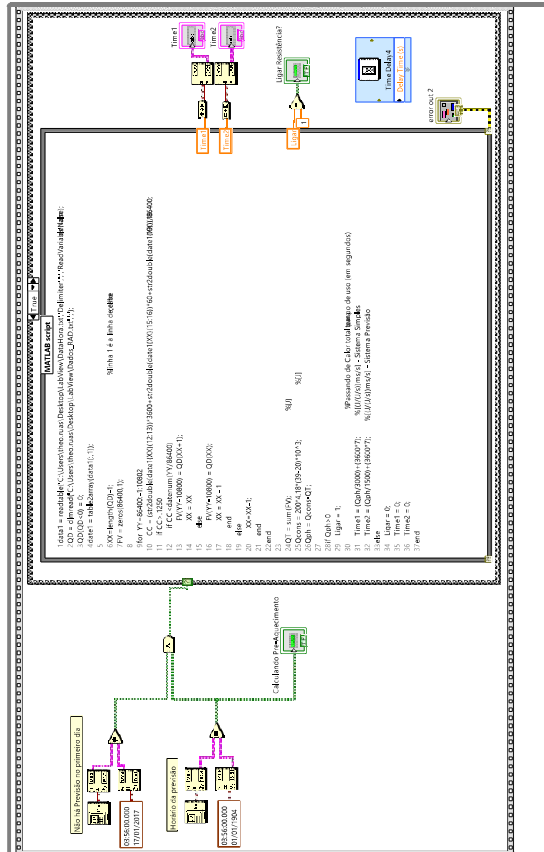


Figura 61 – Control Strategy.

On figure 61 is the programmed Matlab script for the control strategy. In this picture the equal days program is written.

On figure 62 is the programmed clock, and timers that controls the whole program.

And, on figure 63, is the control procedure of the Solenoid Valves applying the Buonavita hot water consumption profile for the Arduino board.

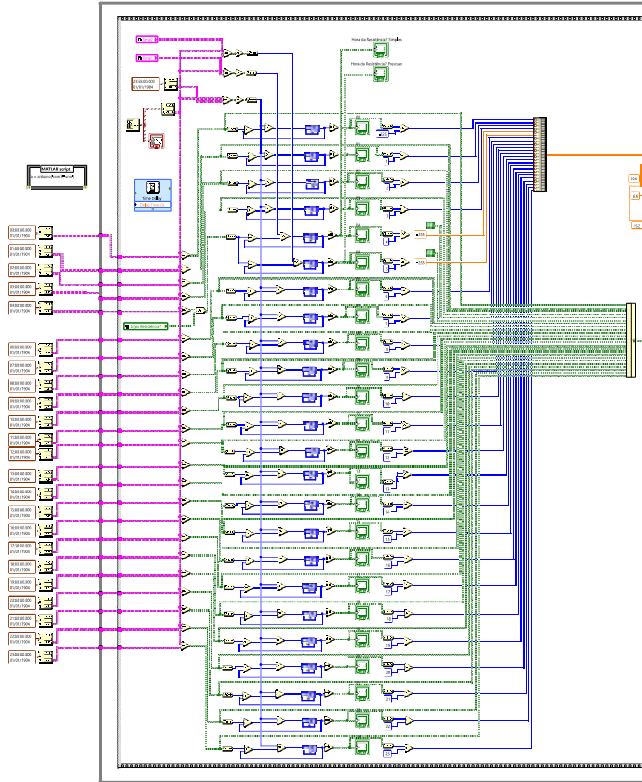


Figura 62 – System Clock.

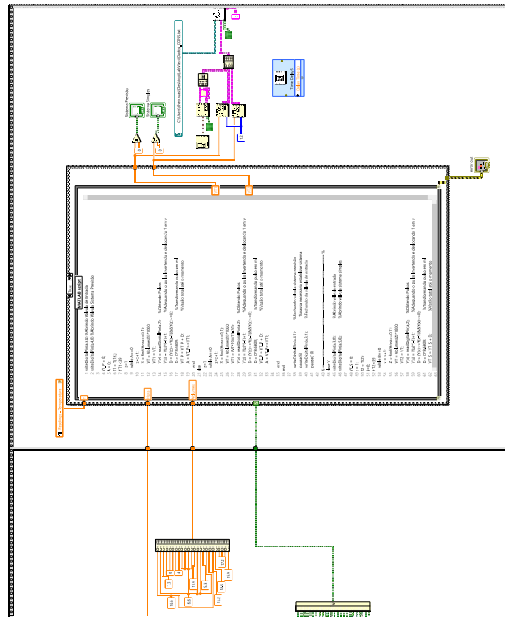


Figura 63 – Control procedure of the Arduino control board.





**ANEXO A - Temperature Transducers Calibration by  
Oestreich (2017)**



A calibração dos seis termorresistores do tipo PT-100 foi realizada por meio da fonte calibração CL134, da marca OMEGA, onde os sensores foram calibrados a partir de uma temperatura de referência gerada pelo calibrador. Foram realizadas 100 medições para cada uma das temperaturas de referência. A faixa de calibração utilizada foi entre 30°C e 65 °C, variando-se a temperatura a cada 5°C.

A média dos valores adquiridos na calibração dos termorresistores do tipo PT-100 é apresentada na Tabela A1, o valor dos desvios padrões para as medições realizadas é apresentado na Tabela A2 e a equação do polinômio de ajuste é visto na Tabela A3.

Tabela A1 – Média dos valores para os termorresistores PT-100:01, 02, 03, 04, 05, 06.

| $T_{ref}$ [ C] | 01    | 02    | 03    | 04    | 05    | 06    | 07    | 08    |
|----------------|-------|-------|-------|-------|-------|-------|-------|-------|
| 30             | 30,07 | 29,79 | 30,08 | 30,02 | 29,98 | 29,74 | 30,96 | 29,76 |
| 35             | 35,05 | 34,57 | 35,04 | 35,01 | 34,95 | 34,43 | 35,33 | 34,51 |
| 40             | 40,06 | 39,41 | 40,01 | 40,02 | 39,95 | 39,24 | 40,19 | 39,35 |
| 45             | 45,06 | 44,25 | 44,99 | 45,02 | 44,94 | 44,04 | 45,10 | 44,17 |
| 50             | 50,04 | 49,09 | 49,94 | 50,01 | 49,91 | 48,84 | 50,09 | 48,98 |
| 55             | 54,99 | 53,92 | 54,87 | 54,97 | 54,86 | 53,63 | 54,94 | 53,77 |
| 60             | 59,96 | 58,85 | 59,81 | 59,95 | 59,85 | 58,40 | 59,83 | 58,48 |
| 65             | 64,93 | 63,73 | 64,75 | 64,92 | 64,84 | 63,27 | 64,68 | 63,12 |

Tabela A2 – Desvio padrão para os termorresistores PT-100:01, 02, 03, 04, 05, 06.

| $T_{ref}$ [ C] | 01    | 02    | 03    | 04    | 05    | 06    | 07    | 08    |
|----------------|-------|-------|-------|-------|-------|-------|-------|-------|
| 30             | 0,026 | 0,018 | 0,024 | 0,023 | 0,023 | 0,020 | 0,022 | 0,019 |
| 35             | 0,026 | 0,017 | 0,024 | 0,024 | 0,023 | 0,018 | 0,022 | 0,017 |
| 40             | 0,025 | 0,015 | 0,022 | 0,021 | 0,021 | 0,015 | 0,020 | 0,015 |
| 45             | 0,054 | 0,028 | 0,037 | 0,031 | 0,03  | 0,041 | 0,040 | 0,030 |
| 50             | 0,036 | 0,031 | 0,032 | 0,031 | 0,030 | 0,041 | 0,031 | 0,036 |
| 55             | 0,031 | 0,034 | 0,025 | 0,025 | 0,025 | 0,048 | 0,037 | 0,045 |
| 60             | 0,021 | 0,013 | 0,016 | 0,017 | 0,018 | 0,020 | 0,035 | 0,017 |
| 65             | 0,028 | 0,044 | 0,023 | 0,024 | 0,023 | 0,046 | 0,031 | 0,048 |

Tabela A3– Coeficientes das curvas de calibração obtidas para cada termorresistor PT-100.

| Sensor | alpha  | beta    |
|--------|--------|---------|
| 01     | 1,004  | -0,2156 |
| 02     | 1,031  | -0,6541 |
| 03     | 1,0094 | -0,3861 |
| 04     | 1,0029 | -0,133  |
| 05     | 1,0043 | -0,1184 |
| 06     | 1,0426 | -0,9268 |
| 07     | 1,0305 | -1,5936 |
| 08     | 1,0461 | -1,166  |